

Novel Higgs-to-125 GeV Higgs boson decays in the complex NMSSM

Shoaib Munir*

National Centre for Nuclear Research, Hoza 69, 00-681 Warsaw, Poland

March 16, 2019

Abstract

In the Next-to-Minimal Supersymmetric Standard Model (NMSSM) a variety of parameter configurations yields a Higgs boson consistent with the one observed at the LHC. Additionally, the Higgs sector of the model can contain explicit CP-violating phases even at the tree level, in contrast with the Minimal Supersymmetric Standard Model (MSSM). In this article we present the complete one-loop Higgs boson mass matrix of the complex NMSSM in the renormalisation-group improved effective potential approach. We also present the trilinear Higgs boson self-couplings and the complete set of expressions for various partial decay widths of a generic CP-mixed Higgs boson in the model. We then analyse a very interesting phenomenological scenario wherein the decay of a relatively light pseudoscalar-like Higgs boson into ~ 125 GeV SM-like Higgs boson(s) is induced by non-zero CP-violating phases. We discuss in detail a few benchmark cases in which such a decay can contribute significantly to the production of SM-like Higgs bosons at the LHC on top of the gluon fusion process. It can thus be partially responsible for the $\gamma\gamma$ excess near 125 GeV due to the subsequent decay of the SM-like Higgs boson. Such a scenario is extremely difficult to realize in the complex MSSM and, if probed at the LHC, it could provide an indication of the non-minimal nature of supersymmetry.

1 Introduction

The new particle with mass around 125 GeV first observed by the CMS and ATLAS experimental collaborations at the Large Hadron Collider (LHC) in July 2012 [1, 2] seems to be increasingly consistent with the Higgs boson of the Standard Model (SM) [3, 4, 5]. However, there is growing evidence from other collider experiments as well as from astroparticle physics and cosmology that the SM fails to provide a complete description of nature and that there must lie physics beyond it. One of the most important yet unresolved issues in particle physics is that of CP violation. Although it was first discovered experimentally in [6] many decades ago, its only source in the SM [7] does not prove sufficient to explain the observed baryon asymmetry in the universe. Therefore, a variety of sources of CP violation beyond the SM have been proposed in literature (for a review, see [8] and references therein), but these remain hidden to this day.

In models with supersymmetry (SUSY), the soft masses and couplings of the superpartners of SM particles as well as the soft Higgs sector parameters can very well be complex and can thus explain the observed CP violation in nature. The Higgs sector of the Minimal Supersymmetric

*From 1st of November, 2013, at Department of Physics and Astronomy, Uppsala University, Box 516, SE-751 20 Uppsala, Sweden.
email: shoaib.munir@physics.uu.se

Standard Model (MSSM) does not contain CP-violating (CPV) phases at the tree level and these are only induced at the one-loop level by the sfermion sector [9, 10, 11, 12, 13, 14, 15, 16]. These phases can substantially modify both the mass spectrum and production/decay rates of the Higgs bosons [17, 18, 19, 20, 21, 22, 23] and can at the same time provide a solution to electroweak baryogenesis [24]. However, these phases are also strongly constrained by the measurements of fermionic Electric Dipole Moments (EDMs) [25, 26, 27]. In the context of the LHC, the impact of the CPV phases on the phenomenology of the MSSM Higgs bosons was studied in detail in [28, 29, 30, 31, 32, 33, 34] prior to the Higgs boson discovery and has been revisited in [35] afterwards.

In the Next-to-Minimal Supersymmetric Standard Model (NMSSM) [36, 37] (see, e.g., [38, 39] for reviews) the presence of an additional Higgs singlet field besides the two MSSM doublets has some very interesting phenomenological implications. In this model either of the two lightest CP-even Higgs bosons, h_1 and h_2 , can play the role of the observed SM-like Higgs boson with mass around 125 GeV [40]. In fact in the NMSSM it is also possible to have h_1 and h_2 almost degenerate in mass around 125 GeV [41], so that the observed signal is actually a superposition of two individual peaks due to each of these, and likewise for h_1 and a_1 , the lightest pseudoscalar of the model [42]. In addition, the model contains some new couplings in the Higgs sector which, if assumed to be complex, can result in new CPV phases even at the tree level, conversely to the MSSM. Indeed, additional MSSM-like phases also appear in the Higgs boson mass matrix beyond the born approximation.

Non-zero CPV phases can substantially modify the phenomenology of the ~ 125 GeV SM-like Higgs boson in the NMSSM, as studied recently in [43]. But, like the MSSM, the measurements of fermionic EDMs can put strong constraints on the allowed values of the CPV phases in the NMSSM also. However, the conditions under which these EDM constraints can be avoided in the MSSM [11, 13, 44] in fact also apply in this model. One can, for example, assign very heavy soft masses to the sfermions of the first two generations in order to minimize their contribution to the EDMs. Alternatively, one can argue that the phase combinations occurring in the EDMs can be different from the ones inducing Higgs boson mixing [45, 46, 47, 48, 49].

The neutral Higgs sector of the complex NMSSM has previously been studied in detail in [50, 51, 52] in the renormalisation-group (RG) improved effective potential approach, including only the dominant one-loop corrections from the (s)quark and gauge sectors. In [53] the complete one-loop Higgs mass matrix has been derived in the Feynman diagrammatic approach. In this article, we provide the complete RG improved one-loop Higgs mass matrix of the cNMSSM in the effective potential approach, in which corrections from third generation (s)quark, stau, gauge as well as chargino/neutralino sectors have been included. We also present the tree level expression for the trilinear Higgs boson self-couplings in the cNMSSM which are hitherto not available in literature. These couplings are extremely important for studying the LHC phenomenology of Higgs bosons in the model. Moreover, we present the complete set of expressions for all possible partial decay widths of a CPV Higgs boson.

We then analyse a very interesting scenario made possible only by non-zero CPV phases in the NMSSM, owing to the fact that the five neutral Higgs bosons of the model no longer carry definite CP-assignments. Thus the scalars and pseudoscalars of the CP-conserving (CPC) limit couple to one another, which implies that any of these Higgs bosons can have a non-zero decay width into a pair of lighter ones, when kinematically allowed. We argue that such a scenario can be of particular importance in the context of the recent LHC discovery. The reason is that it is very much probable for the lighter of the two pseudoscalar-like Higgs bosons to have a mass ~ 250 GeV, particularly when one of the scalar-like Higgs boson is required to have SM-like $\gamma\gamma$ and ZZ signal rates and a mass near 125 GeV. Such a mass would result in its having a much larger branching ratio (BR) into a pair of the SM-like Higgs bosons compared to that of the other, typically much heavier,

scalar-like Higgs bosons despite a relatively much smaller trilinear coupling.

However, despite having a large BR into lighter Higgs bosons, the above mentioned ~ 250 GeV boson can be very difficult to produce at the LHC on account of being pseudoscalar-like and thus having a considerably reduced coupling to two gluons. Therefore, the relative probability of its production in the gluon fusion mode also needs to be taken into account in the above scenario. For this purpose, we define an auxiliary signal rate, similar to the conventional ‘reduced cross section’, which quantifies the contribution of the ~ 250 GeV boson to the production of the SM-like Higgs bosons, decaying eventually into photons pairs, at the LHC. We then select representative points from three distinct regions in the cNMSSM parameter space wherein the ~ 125 GeV SM-like Higgs boson is either h_1 or h_2 , the lightest and next-to-lightest of the five Higgs bosons, respectively, to investigate our scenario of interest. We discuss in detail the impact of the variation in the most relevant of the CPV phases on our auxiliary signal rate in each of these cases. We conclude that for large values of the phase, this rate can become quite significant, reaching a few tens of percents of the direct production rate of the SM-like Higgs boson in the gluon fusion channel.

The article is organised as follows. In the next section we will give details of the cNMSSM Higgs mass matrix at the tree level and the complete set of one-loop as well as logarithmically enhanced dominant two-loop corrections to it. In Sect. 3 we will present the expressions for the trilinear self-couplings of the Higgs bosons and will also define notation for their couplings to other model particles. In Sect. 4 we will provide detailed expressions for all possible two-body partial decay widths of the Higgs boson in the presence of CPV phases will be provided. In Sect. 5, after discussing at length our scenario of interest, we will present our numerical results for the three points investigated. We will summarise our findings in Sect. 6.

2 Higgs sector of the cNMSSM

As noted in the introduction, the NMSSM contains a singlet Higgs superfield, \hat{S} , besides the two MSSM $SU(2)_L$ doublet superfields,

$$\hat{H}_u = \begin{pmatrix} \hat{H}_u^+ \\ \hat{H}_u^0 \end{pmatrix}, \quad \hat{H}_d = \begin{pmatrix} \hat{H}_d^0 \\ \hat{H}_d^- \end{pmatrix}. \quad (1)$$

The scale-invariant superpotential of the cNMSSM is thus written as

$$W_{\text{NMSSM}} = \text{MSSM Yukawa terms} + \lambda \hat{S} \hat{H}_u \hat{H}_d + \frac{\kappa}{3} \hat{S}^3, \quad (2)$$

where $\lambda \equiv |\lambda|e^{i\phi_\lambda}$ and $\kappa \equiv |\kappa|e^{i\phi_\kappa}$ are dimensionless complex Yukawa couplings. The second term in the above superpotential replaces the Higgs-higgsino mass term, $\mu \hat{H}_u \hat{H}_d$, of the MSSM superpotential and the last cubic term explicitly breaks the dangerous $U(1)_{PQ}$ symmetry, introducing in turn a discrete Z_3 symmetry. Upon breaking of the electroweak symmetry, the singlet field acquires a vacuum expectation value (TeV), s , naturally of the order of the SUSY-breaking scale, M_{SUSY} , and an effective μ -term, $\mu_{\text{eff}} = \lambda s$, is generated.

2.1 Tree level Higgs potential and mass matrix

The superpotential in eq. (2) leads to the tree level Higgs potential containing the D -, F - and soft SUSY-breaking terms:

$$\begin{aligned}
V_0 = & \left| \lambda (H_u^+ H_d^- - H_u^0 H_d^0) + \kappa S^2 \right|^2 \\
& + \left(m_{H_u}^2 + |\mu + \lambda S|^2 \right) \left(|H_u^0|^2 + |H_u^+|^2 \right) + \left(m_{H_d}^2 + |\mu + \lambda S|^2 \right) \left(|H_d^0|^2 + |H_d^-|^2 \right) \\
& + \frac{g^2}{4} \left(|H_u^0|^2 + |H_u^+|^2 - |H_d^0|^2 - |H_d^-|^2 \right)^2 + \frac{g_2^2}{2} |H_u^+ H_d^{0*} + H_u^0 H_d^{-*}|^2 \\
& + m_S^2 |S|^2 + (\lambda A_\lambda (H_u^+ H_d^- - H_u^0 H_d^0) S + \frac{1}{3} \kappa A_\kappa S^3 + \text{h.c.}), \tag{3}
\end{aligned}$$

where $g^2 \equiv \frac{g_1^2 + g_2^2}{2}$, with g_1 and g_2 being the $U(1)_Y$ and $SU(2)_L$ gauge couplings, respectively, and $A_\lambda \equiv |A_\lambda| e^{i\phi_{A_\lambda}}$ and $A_\kappa \equiv |A_\kappa| e^{i\phi_{A_\kappa}}$ are dimensionful soft SUSY-breaking trilinear couplings. In order to obtain the physical Higgs states the above potential is expanded around the VEVs of the three Higgs fields as

$$\begin{aligned}
H_d^0 &= \begin{pmatrix} \frac{1}{\sqrt{2}} (v_d + H_{dR} + i H_{dI}) \\ H_d^- \end{pmatrix}, \\
H_u^0 &= e^{i\theta} \begin{pmatrix} H_u^+ \\ \frac{1}{\sqrt{2}} (v_u + H_{uR} + i H_{uI}) \end{pmatrix}, \\
S &= \frac{e^{i\varphi}}{\sqrt{2}} (s + S_R + i S_I). \tag{4}
\end{aligned}$$

The potential in eq. (3) then has a minimum at non-vanishing v_u , v_d and s only if the following so-called tadpole conditions are satisfied:

$$\begin{aligned}
\frac{1}{v_d} \left\langle \frac{\partial V_0}{\partial H_{dR}} \right\rangle &= m_{H_d}^2 + \frac{g^2}{4} (v_d^2 - v_u^2) - R_\lambda \frac{v_u s}{v_d} + \frac{|\lambda|^2}{2} (v_u^2 + s^2) - \frac{1}{2} \mathcal{R} \frac{v_u s^2}{v_d} = 0, \\
\frac{1}{v_u} \left\langle \frac{\partial V_0}{\partial H_{uR}} \right\rangle &= m_{H_u}^2 - \frac{g^2}{4} (v_d^2 - v_u^2) - R_\lambda \frac{v_d s}{v_u} + \frac{|\lambda|^2}{2} (v_d^2 + s^2) - \frac{1}{2} \mathcal{R} \frac{v_d s^2}{v_u} = 0, \\
\frac{1}{s} \left\langle \frac{\partial V_0}{\partial S_R} \right\rangle &= m_S^2 - R_\lambda \frac{v_d v_u}{s} + \frac{|\lambda|^2}{2} (v_d^2 + v_u^2) + |\kappa|^2 s^2 - \mathcal{R} v_d v_u + R_\kappa s = 0, \tag{5}
\end{aligned}$$

$$\begin{aligned}
\frac{1}{v_u} \left\langle \frac{\partial V_0}{\partial H_{dI}} \right\rangle &= \frac{1}{v_d} \left\langle \frac{\partial V_0}{\partial H_{uI}} \right\rangle = I_\lambda s + \frac{1}{2} \mathcal{I} s^2 = 0, \\
\frac{1}{s} \left\langle \frac{\partial V_0}{\partial S_I} \right\rangle &= I_\lambda \frac{v_d v_u}{s} - \mathcal{I} v_d v_u - I_\kappa s = 0, \tag{6}
\end{aligned}$$

where we have defined

$$\begin{aligned}
\mathcal{R} &= |\lambda| |\kappa| \cos(\phi'_\lambda - \phi'_\kappa), & \mathcal{I} &= |\lambda| |\kappa| \sin(\phi'_\lambda - \phi'_\kappa), \\
R_\lambda &= \frac{|\lambda| |A_\lambda|}{\sqrt{2}} \cos(\phi'_\lambda + \phi_{A_\lambda}), & R_\kappa &= \frac{|\kappa| |A_\kappa|}{\sqrt{2}} \cos(\phi'_\kappa + \phi_{A_\kappa}), \\
I_\lambda &= \frac{|\lambda| |A_\lambda|}{\sqrt{2}} \sin(\phi'_\lambda + \phi_{A_\lambda}), & I_\kappa &= \frac{|\kappa| |A_\kappa|}{\sqrt{2}} \sin(\phi'_\kappa + \phi_{A_\kappa}), \tag{7}
\end{aligned}$$

with

$$\phi'_\lambda \equiv \phi_\lambda + \theta + \varphi \quad \text{and} \quad \phi'_\kappa \equiv \phi_\kappa + 3\varphi. \quad (8)$$

The parameters I_λ and I_κ can be re-expressed in terms of \mathcal{I} using the CP-odd tadpole conditions in eq. (6) as

$$I_\lambda = -\frac{1}{2}\mathcal{I}s, \quad I_\kappa = -\frac{3}{2}\mathcal{I}\frac{v_d v_u}{s}. \quad (9)$$

Then the phase combinations $\phi'_\lambda + \phi_{A_\lambda}$ and $\phi'_\kappa + \phi_{A_\kappa}$ are determined up to a twofold ambiguity by $\phi'_\lambda - \phi'_\kappa$, which is thus the only remaining physical CP phase at the tree level. The three CP-even tadpole conditions in eq. (5), on the other hand, can be used to remove the soft mass parameters $m_{H_u}^2$, $m_{H_d}^2$, and m_S^2 .

The 6×6 neutral Higgs mass matrix, obtained by taking the second derivative of the potential in Eq. (3) evaluated at the vacuum, can be cast into the form:

$$\mathcal{M}_0^2 = \begin{pmatrix} \mathcal{M}_S^2 & \mathcal{M}_{SP}^2 \\ (\mathcal{M}_{SP}^2)^T & \mathcal{M}_P^2 \end{pmatrix}, \quad (10)$$

in the basis $\mathbf{H}^T = (H_{dR}, H_{uR}, S_R, H_{dI}, H_{uI}, S_I)$. The elements of the top left 3×3 CP-even block in the above equation are given as

$$\begin{aligned} \mathcal{M}_{S,11}^2 &= \frac{g^2}{2}v_d^2(Q) + \left(R_\lambda + \frac{\mathcal{R}s(Q)}{2}\right)s(Q)\tan\beta, \\ \mathcal{M}_{S,22}^2 &= \frac{g^2}{2}v_u^2(Q) + \left(R_\lambda + \frac{\mathcal{R}s(Q)}{2}\right)\frac{s(Q)}{\tan\beta}, \\ \mathcal{M}_{S,33}^2 &= R_\lambda\frac{v_d(Q)v_u(Q)}{s(Q)} + 2|\kappa|^2s(Q)^2 + R_\kappa s(Q), \\ \mathcal{M}_{S,12}^2 &= (\mathcal{M}_{S,21}^2) = \left(-\frac{g_1^2 + g_2^2}{4} + |\lambda|^2\right)v_d(Q)v_u(Q) - \left(R_\lambda + \frac{\mathcal{R}s(Q)}{2}\right)s(Q), \\ \mathcal{M}_{S,13}^2 &= (\mathcal{M}_{S,31}^2) = -R_\lambda v_u(Q) + |\lambda|^2 v_d(Q)s(Q) - \mathcal{R}v_u(Q)s(Q), \\ \mathcal{M}_{S,23}^2 &= (\mathcal{M}_{S,32}^2) = -R_\lambda v_d(Q) + |\lambda|^2 v_u(Q)s(Q) - \mathcal{R}v_d(Q)s(Q), \end{aligned} \quad (11)$$

where $v_u(Q)$, $v_d(Q)$ and $s(Q)$ are the three Higgs VEVs defined at the scale $Q^2 = M_{\text{SUSY}}^2$ and $\tan\beta \equiv v_u(Q)/v_d(Q)$. The bottom right CP-odd block in eq. (10) is given as

$$\begin{aligned} \mathcal{M}_{P,11}^2 &= \left(R_\lambda + \frac{\mathcal{R}s(Q)}{2}\right)s(Q)\tan\beta, \\ \mathcal{M}_{P,22}^2 &= \left(R_\lambda + \frac{\mathcal{R}s(Q)}{2}\right)\frac{s(Q)}{\tan\beta}, \\ \mathcal{M}_{P,33}^2 &= R_\lambda\frac{v_d(Q)v_u(Q)}{s(Q)} + 2\mathcal{R}v_d(Q)v_u(Q) - 3R_\kappa s(Q), \\ \mathcal{M}_{P,12}^2 &= (\mathcal{M}_{P,21}^2) = \left(R_\lambda + \frac{\mathcal{R}s(Q)}{2}\right)s(Q), \\ \mathcal{M}_{S,13}^2 &= (\mathcal{M}_{S,31}^2) = (R_\lambda - \mathcal{R}s(Q))v_u(Q), \\ \mathcal{M}_{S,23}^2 &= (\mathcal{M}_{S,32}^2) = (R_\lambda - \mathcal{R}s(Q))v_d(Q), \end{aligned} \quad (12)$$

and the off-diagonal CP-mixing block reads

$$\mathcal{M}_{SP}^2 = \begin{pmatrix} 0 & 0 & -\frac{3}{2}\mathcal{I}s v_u \\ 0 & 0 & -\frac{3}{2}\mathcal{I}s v_d \\ \frac{1}{2}\mathcal{I}s v_u & \frac{1}{2}\mathcal{I}s v_d & 2\mathcal{I}v_d v_u \end{pmatrix}. \quad (13)$$

2.2 RG improved one-loop effective potential

The one-loop corrections to the effective potential are given by the Coleman-Weinberg formula (in the $\overline{\text{DR}}$ scheme with an ultraviolet cutoff M_{SUSY}^2) as

$$\Delta V_{\text{eff}} = \frac{1}{64\pi^2} \text{STr } M^4 \left[\ln \left(\frac{M^2}{M_{\text{SUSY}}^2} \right) - \frac{3}{2} \right]. \quad (14)$$

As a result of these corrections the Higgs mass matrix gets modified so that

$$\mathcal{M}_H^2 = \mathcal{M}_0^2 + \Delta \mathcal{M}_{\text{eff}}^2. \quad (15)$$

In the following we present analytical expressions for the corrections $\Delta \mathcal{M}_{\text{eff}}^2$ above. These corrections have been adopted from [38] and modified to explicitly include the CPV phases. They are thus of the same order as those implemented in the publicly available package NMSSMTools-v3.2.4 [54].

2.2.1 Top and bottom squark contributions

Some of the radiative corrections due to the stop and sbottom loops can be accounted for by the following shift in the Higgs mass matrix:

$$A_\lambda \rightarrow A'_\lambda = A_\lambda + \frac{3h_t^2}{16\pi^2} A_t f_t + \frac{3h_b^2}{16\pi^2} A_b f_b, \quad (16)$$

where h_t and h_b are the Yukawa couplings of top and bottom quarks and $A_t \equiv |A_t|e^{i\phi_{A_t}}$ and $A_b \equiv |A_b|e^{i\phi_{A_b}}$ are their soft SUSY-breaking counterparts for the top and bottom squarks, respectively. The above shift results in the redefinition of the parameters \mathcal{R} and \mathcal{I} given in eq. (7) and a subsequent improvement in the relation between the latter and I_λ given in eq. (9). It also takes care of the only radiative corrections, $\sim h_{t,b}^4$, to \mathcal{M}_P^2 . The remaining corrections $\sim h_t^2 \equiv h_t^2(M_{\text{SUSY}}^2)$ and $\sim h_b^2 \equiv h_b^2(M_{\text{SUSY}}^2)$ to \mathcal{M}_S^2 are written as

$$\begin{aligned} \Delta \mathcal{M}_{S,11}^2 &= \frac{3h_b^2 m_b^2}{8\pi^2} \left(-|A_b|^2 B'_b g_b + 2|A_b|B_b L_{\bar{b}} + L_{b\bar{b}} \right) - \frac{3h_t^2 m_t^2}{8\pi^2} |\mu|^2 B'_t g_t, \\ \Delta \mathcal{M}_{S,22}^2 &= \frac{3h_t^2 m_t^2}{8\pi^2} \left(-|A_t|^2 B'_t g_t + 2|A_t|B_t L_{\bar{t}} + L_{t\bar{t}} \right) - \frac{3h_b^2 m_b^2}{8\pi^2} |\mu|^2 B'_b g_b, \\ \Delta \mathcal{M}_{S,33}^2 &= -\frac{3h_t^2 m_t^2}{16\pi^2} |\lambda|^2 v_d^2(Q) B'_t g_t - \frac{3h_b^2 m_b^2}{16\pi^2} |\lambda|^2 v_u^2(Q) B'_b g_b, \\ \Delta \mathcal{M}_{S,12}^2 &= \frac{3h_t^2 m_t^2}{8\pi^2} |\mu| \left(|A_t| B'_t g_t \cos(\phi'_\lambda + \phi_{A_t}) - \frac{|A_t| \cos(\phi'_\lambda + \phi_{A_t}) + |\mu| \cot \beta}{m_{\tilde{t}_2^2} - m_{\tilde{t}_1^2}} \right) \\ &\quad + \frac{3h_b^2 m_b^2}{8\pi^2} |\mu| \left(|A_b| B'_b g_b \cos(\phi'_\lambda + \phi_{A_b}) - \frac{|A_b| \cos(\phi'_\lambda + \phi_{A_b}) + |\mu| \tan \beta}{m_{\tilde{b}_2^2} - m_{\tilde{b}_1^2}} \right), \\ \Delta \mathcal{M}_{S,13}^2 &= \frac{3h_b^2 m_b^2 |\lambda| v_u(Q)}{8\sqrt{2}\pi^2} \left(|A_b| B'_b g_b \cos(\phi'_\lambda + \phi_{A_b}) - \frac{|A_b| \cos(\phi'_\lambda + \phi_{A_b}) + |\mu| \tan \beta}{m_{\tilde{b}_2^2} - m_{\tilde{b}_1^2}} \right) \\ &\quad + \frac{3h_t^2}{64\pi^2} |\lambda|^2 s(Q) v_d(Q) (4f_t - 4m_t^2 B'_t g_t), \\ \Delta \mathcal{M}_{S,23}^2 &= \frac{3h_t^2 m_t^2 |\lambda| v_d(Q)}{8\sqrt{2}\pi^2} \left(|A_t| B'_t g_t \cos(\phi'_\lambda + \phi_{A_t}) - \frac{|A_t| \cos(\phi'_\lambda + \phi_{A_t}) + |\mu| \cot \beta}{m_{\tilde{t}_2^2} - m_{\tilde{t}_1^2}} \right) \\ &\quad + \frac{3h_b^2}{64\pi^2} |\lambda|^2 s(Q) v_u(Q) (4f_b - 4m_b^2 B'_b g_b), \end{aligned} \quad (17)$$

where $|\mu| \equiv |\mu_{\text{eff}}|/\sqrt{2} = |\lambda|s(Q)/\sqrt{2}$, m_t and m_b are the masses of t and b quarks, respectively, and the squark masses $m_{\tilde{q}}$ are given in Appendix A. Also in the above equations

$$\begin{aligned} B_t &= \frac{|A_t| - |\mu| \cot \beta \cos(\phi'_\lambda + \phi_{A_t})}{m_{\tilde{t}_2^2} - m_{\tilde{t}_1^2}}, \quad B_b = \frac{|A_b| - |\mu| \tan \beta \cos(\phi'_\lambda + \phi_{A_b})}{m_{\tilde{b}_2^2} - m_{\tilde{b}_1^2}}, \\ B'_t &= \frac{|A_t|^2 + |\mu|^2 \cot^2 \beta - 2|\mu||A_t| \cot \beta \cos(\phi'_\lambda - \phi_{A_t})}{(m_{\tilde{t}_2^2} - m_{\tilde{t}_1^2})^2}, \\ B'_b &= \frac{|A_b|^2 + |\mu|^2 \tan^2 \beta - 2|\mu||A_b| \tan \beta \cos(\phi'_\lambda - \phi_{A_b})}{(m_{\tilde{b}_2^2} - m_{\tilde{b}_1^2})^2}, \end{aligned} \quad (18)$$

and the quantities $L_{\tilde{f}}, L_{\tilde{f}f}, f_f$ and g_f are given in Appendix B. \mathcal{M}_{SP}^2 also receives the corresponding corrections given as

$$\begin{aligned} \Delta \mathcal{M}_{SP,11}^2 &= -\frac{3h_b^2 m_b^2}{4\pi^2} \frac{|A_b||\mu| \tan \beta \sin(\phi'_\lambda + \phi_{A_b})}{m_{\tilde{b}_2^2} - m_{\tilde{b}_1^2}} L_{\tilde{b}}, \\ \Delta \mathcal{M}_{SP,22}^2 &= -\frac{3h_t^2 m_t^2}{4\pi^2} \frac{|A_t||\mu| \cot \beta \sin(\phi'_\lambda + \phi_{A_t})}{m_{\tilde{t}_2^2} - m_{\tilde{t}_1^2}} L_{\tilde{t}}, \\ \Delta \mathcal{M}_{SP,12}^2 &= \frac{3h_t^2 m_t^2}{8\pi^2} |\mu| \left(|A_t| B'_t g_t \sin(\phi'_\lambda + \phi_{A_t}) - \frac{|A_t| \sin(\phi'_\lambda + \phi_{A_t})}{m_{\tilde{t}_2^2} - m_{\tilde{t}_1^2}} \right) \\ &\quad + \frac{3h_b^2 m_b^2}{8\pi^2} |\mu| \left(|A_b| B'_b g_b \sin(\phi'_\lambda + \phi_{A_b}) - \frac{|A_b| \sin(\phi'_\lambda + \phi_{A_b})}{m_{\tilde{b}_2^2} - m_{\tilde{b}_1^2}} \right), \\ \Delta \mathcal{M}_{SP,13}^2 &= \frac{3h_b^2 m_b^2 |\lambda| v_u(Q)}{8\sqrt{2}\pi^2} \left(|A_b| B'_b g_b \sin(\phi'_\lambda + \phi_{A_b}) - \frac{|A_b| \sin(\phi'_\lambda + \phi_{A_b})}{m_{\tilde{b}_2^2} - m_{\tilde{b}_1^2}} \right), \\ \Delta \mathcal{M}_{SP,23}^2 &= \frac{3h_t^2 m_t^2 |\lambda| v_d(Q)}{8\sqrt{2}\pi^2} \left(|A_t| B'_t g_t \sin(\phi'_\lambda + \phi_{A_t}) - \frac{|A_t| \sin(\phi'_\lambda + \phi_{A_t})}{m_{\tilde{t}_2^2} - m_{\tilde{t}_1^2}} \right). \end{aligned} \quad (19)$$

There are additional D -term contributions which are quite involved but do not give large logarithms since the squarks are assumed to have masses close to the ultraviolet cutoff M_{SUSY}^2 . These corrections are given for \mathcal{M}_S^2 as

$$\begin{aligned} \Delta \mathcal{M}_{S,11}^2 &= 2|\mu| \left(|A_t| C_t \cot \beta \cos(\phi'_\lambda + \phi_{A_t}) - |A_b| C_b \tan \beta \cos(\phi'_\lambda + \phi_{A_b}) \right) \\ &\quad + 2|A_b|^2 C_b + 2D_b - 2|\mu|^2 C_t \cot^2 \beta, \\ \Delta \mathcal{M}_{S,22}^2 &= 2|\mu| \left(|A_b| C_b \tan \beta \cos(\phi'_\lambda + \phi_{A_b}) - |A_t| C_t \cot \beta \cos(\phi'_\lambda + \phi_{A_t}) \right) \\ &\quad + 2|A_t|^2 C_t + 2D_t - 2|\mu|^2 C_b \tan^2 \beta, \\ \Delta \mathcal{M}_{S,12}^2 &= \cot \beta \left((|\mu|^2 - |A_t|^2) C_t - D_t \right) + \tan \beta \left((|\mu|^2 - |A_b|^2) C_b - D_b \right) \\ &\quad - |\mu| \left(|A_t| C_t (1 - \cot^2 \beta) \cos(\phi'_\lambda + \phi_{A_t}) + |A_b| C_b (1 - \tan^2 \beta) \cos(\phi'_\lambda + \phi_{A_b}) \right), \\ \Delta \mathcal{M}_{S,13}^2 &= \frac{|\lambda|}{\sqrt{2}} \left(|A_t| C_t v_d(Q) \cot \beta \cos(\phi'_\lambda + \phi_{A_t}) - |A_b| C_b v_u(Q) \cos(\phi'_\lambda + \phi_{A_b}) \right) \\ &\quad + \frac{|\lambda|^2}{2} s(Q) \left(v_u(Q) C_b \tan \beta - v_d(Q) C_t \cot \beta \right), \\ \Delta \mathcal{M}_{S,23}^2 &= \frac{|\lambda|}{\sqrt{2}} \left(|A_b| C_b v_u(Q) \tan \beta \cos(\phi'_\lambda + \phi_{A_b}) - |A_t| C_t v_d(Q) \cos(\phi'_\lambda + \phi_{A_t}) \right) \\ &\quad + \frac{|\lambda|^2}{2} s(Q) \left(v_d(Q) C_t \cot \beta - v_u(Q) C_b \tan \beta \right), \end{aligned} \quad (20)$$

where again the quantities C_f and D_f are defined in Appendix B, and for \mathcal{M}_{SP}^2 as

$$\begin{aligned}
\Delta\mathcal{M}_{SP,11}^2 &= 2|\mu|\left(|A_t|C_t \cot\beta \sin(\phi'_\lambda + \phi_{A_t}) - |A_b|C_b \tan\beta \sin(\phi'_\lambda + \phi_{A_b})\right), \\
\Delta\mathcal{M}_{SP,22}^2 &= 2|\mu|\left(|A_b|C_b \tan\beta \sin(\phi'_\lambda + \phi_{A_b}) - |A_t|C_t \cot\beta \sin(\phi'_\lambda + \phi_{A_t})\right), \\
\Delta\mathcal{M}_{SP,12}^2 &= -|\mu|\left(|A_t|C_t(1 - \cot^2\beta) \sin(\phi'_\lambda + \phi_{A_t}) + |A_b|C_b(1 - \tan^2\beta) \sin(\phi'_\lambda + \phi_{A_b})\right), \\
\Delta\mathcal{M}_{SP,13}^2 &= \frac{|\lambda|}{\sqrt{2}}\left(|A_t|C_tv_d \cot\beta \sin(\phi'_\lambda + \phi_{A_t}) - |A_b|C_bv_u \sin(\phi'_\lambda + \phi_{A_b})\right), \\
\Delta\mathcal{M}_{SP,23}^2 &= \frac{|\lambda|}{\sqrt{2}}\left(|A_b|C_bv_u \tan\beta \sin(\phi'_\lambda + \phi_{A_b}) - |A_t|C_tv_d \sin(\phi'_\lambda + \phi_{A_t})\right). \tag{21}
\end{aligned}$$

Finally, neglecting all terms without two powers of large logarithms the dominant two-loop squark contributions to the effective potential can be obtained by integrating the relevant RGEs. These contributions are given as

$$\begin{aligned}
\Delta\mathcal{M}_{S,11}^2 &= \frac{3h_b^4v_d^2(Q)}{256\pi^4}\left(\ln^2\left(\frac{M_{\text{SUSY}}^2}{m_t^2}\right)(16g_3^2 - \frac{2}{3}g_1^2 + 3\sin^2\beta h_t^2 - 3\cos^2\beta h_b^2)\right. \\
&\quad \left.+ \left[\ln^2\left(\frac{M_A^2}{m_t^2}\right) - \ln^2\left(\frac{M_{\text{SUSY}}^2}{m_t^2}\right)\right](3\sin^2\beta h_b^2 + (3\sin^2\beta + 1)h_t^2)\right), \\
\Delta\mathcal{M}_{S,22}^2 &= \frac{3h_t^4v_u^2(Q)}{256\pi^4}\left(\ln^2\left(\frac{M_{\text{SUSY}}^2}{m_t^2}\right)(16g_3^2 + \frac{4}{3}g_1^2 - 3\sin^2\beta h_t^2 + 3\cos^2\beta h_b^2)\right. \\
&\quad \left.+ \left[\ln^2\left(\frac{M_A^2}{m_t^2}\right) - \ln^2\left(\frac{M_{\text{SUSY}}^2}{m_t^2}\right)\right](3\cos^2\beta h_t^2 + (3\cos^2\beta + 1)h_b^2)\right). \tag{22}
\end{aligned}$$

2.2.2 Chargino/neutralino, gauge boson and dominant slepton contributions

Again, some of the radiative corrections due to the chargino/neutralino loops can be described by an additional shift in A_λ on top of the corrections in eq. (16),

$$A'_\lambda \rightarrow A''_\lambda = A'_\lambda + \frac{1}{16\pi^2}(g_1^2 M_1 + 3g_2^2 M_2)L_{M_2\mu}, \tag{23}$$

where M_1 and M_2 are the soft gaugino masses and the logarithm $L_{M_2\mu}$ is defined, along with $L_{\mu\nu}$, L_μ and $L_{\mu\nu}$ used in the following, in Appendix B. For the CP-odd block in the Higgs mass matrix, all the radiative corrections due to chargino/neutralino loops, $\sim g^4$, are included by the above shift. The remaining contributions to \mathcal{M}_S^2 are given as

$$\begin{aligned}
\Delta\mathcal{M}_{S,11}^2 &= \frac{1}{16\pi^2}\left[2g^2m_Z^2\cos^2\beta(-10 + 16\sin^2\theta_W - 8\sin^4\theta_W)L_{M_2\mu}\right. \\
&\quad \left.- 4\left(|\mu|^2\mathcal{R}\tan\beta + \frac{\lambda^4m_Z^2\cos^2\beta}{g^2}\right)L_{\mu\nu}\right], \\
\Delta\mathcal{M}_{S,22}^2 &= \frac{1}{16\pi^2}\left[2g^2m_Z^2\sin^2\beta(-10 + 16\sin^2\theta_W - 8\sin^4\theta_W)L_{M_2\mu}\right. \\
&\quad \left.- 4\left(|\mu|^2\mathcal{R}\cot\beta + \frac{\lambda^4m_Z^2\sin^2\beta}{g^2}\right)L_{\mu\nu}\right], \\
\Delta\mathcal{M}_{S,33}^2 &= \frac{1}{16\pi^2}\left(-32|\kappa|^2\nu^2L_\nu - 8|\lambda|^2|\mu|^2L_\mu\right),
\end{aligned}$$

$$\begin{aligned}
\Delta\mathcal{M}_{S,12}^2 &= \frac{1}{16\pi^2} \left[4 \left(|\mu|^2 \mathcal{R} - \frac{\lambda^4 m_Z^2 \sin \beta \cos \beta}{g^2} \right) L_{\mu\nu} \right. \\
&\quad \left. - 4g^2 m_Z^2 \sin \beta \cos \beta L_{M_2\mu} \right], \\
\Delta\mathcal{M}_{S,13}^2 &= \frac{1}{16\pi^2} \frac{m_Z s(Q)}{\sqrt{g_1^2 + g_2^2}} \left[2|\lambda|^2 g^2 \cos \beta (-6 + 4 \sin^2 \theta_W) L_{M_2\mu} \right. \\
&\quad \left. + 2\sqrt{2} |\lambda|^2 \left(2\mathcal{R} \sin \beta - (|\lambda|^2 + 4|\kappa|^2) \cos \beta \right) L_{\mu\nu} \right], \\
\Delta\mathcal{M}_{S,23}^2 &= \frac{1}{16\pi^2} \frac{m_Z s(Q)}{\sqrt{g_1^2 + g_2^2}} \left[2|\lambda|^2 g^2 \sin \beta (-6 + 4 \sin^2 \theta_W) L_{M_2\mu} \right. \\
&\quad \left. + 2\sqrt{2} |\lambda|^2 \left(2\mathcal{R} \cos \beta - (|\lambda|^2 + 4|\kappa|^2) \sin \beta \right) L_{\mu\nu} \right], \tag{24}
\end{aligned}$$

where $|\nu| \equiv |\kappa|s(Q)/\sqrt{2}$ and m_Z is the mass of Z boson. The corresponding corrections to \mathcal{M}_{SP}^2 are given as

$$\begin{aligned}
\Delta\mathcal{M}_{S,11}^2 &= -\frac{1}{4\pi^2} |\mu|^2 \mathcal{I} \tan \beta L_{\mu\nu}, \\
\Delta\mathcal{M}_{S,22}^2 &= -\frac{1}{4\pi^2} |\mu|^2 \mathcal{I} \cot \beta L_{\mu\nu}, \\
\Delta\mathcal{M}_{S,12}^2 &= \frac{1}{4\pi^2} |\mu|^2 \mathcal{I} L_{\mu\nu}, \\
\Delta\mathcal{M}_{S,13}^2 &= \frac{1}{2\sqrt{2}\pi^2} \frac{m_Z s(Q)}{\sqrt{g_1^2 + g_2^2}} |\lambda|^2 \mathcal{I} \sin \beta L_{\mu\nu}, \\
\Delta\mathcal{M}_{P,23}^2 &= \frac{1}{2\sqrt{2}\pi^2} \frac{m_Z s(Q)}{\sqrt{g_1^2 + g_2^2}} |\lambda|^2 \mathcal{I} \cos \beta L_{\mu\nu}. \tag{25}
\end{aligned}$$

The contributions from gauge bosons can be conveniently written as

$$\begin{aligned}
\Delta\mathcal{M}_{S,11}^2 &= \Delta_{\text{Gauge}} \cos^2 \beta, \\
\Delta\mathcal{M}_{S,22}^2 &= \Delta_{\text{Gauge}} \sin^2 \beta, \\
\Delta\mathcal{M}_{S,12}^2 &= \Delta_{\text{Gauge}} \sin \beta \cos \beta, \tag{26}
\end{aligned}$$

in terms of the auxiliary quantity

$$\Delta_{\text{Gauge}} = \frac{1}{16\pi^2} g^2 m_Z^2 (-9 + 12 \sin^2 \theta_W - 6 \sin^4 \theta_W) \ln \left(\frac{M_{\text{SUSY}}^2}{m_Z^2} \right). \tag{27}$$

Finally, sleptons can be considerably lighter than the squarks and hence can give comparatively larger D -term contributions which are written as

$$\begin{aligned}
\Delta\mathcal{M}_{S,11}^2 &= \Delta_{\tilde{l}} \cos^2 \beta, \\
\Delta\mathcal{M}_{S,22}^2 &= \Delta_{\tilde{l}} \sin^2 \beta, \\
\Delta\mathcal{M}_{S,12}^2 &= -\Delta_{\tilde{l}} \sin \beta \cos \beta, \tag{28}
\end{aligned}$$

where, assuming a common slepton mass, $m_{\tilde{l}}$,

$$\Delta_{\tilde{l}} = -\frac{1}{16\pi^2} g^2 m_Z^2 (9 \sin^4 \theta_W + 3 \cos^4 \theta_W) \ln \left(\frac{M_{\text{SUSY}}^2}{m_{\tilde{l}}^2} \right), \tag{29}$$

with θ_W being the weak mixing angle.

2.2.3 Wave function renormalisation

As mentioned earlier, the elements of the loop-corrected Higgs mass matrix obtained so far contain VeVs $v_u(Q)$, $v_d(Q)$ and $s(Q)$ defined at the scale $Q^2 = M_{\text{SUSY}}^2$. These VeVs are related to the VeVs of the properly normalised Higgs fields (i.e., after the addition of quantum effects with $Q^2 < M_{\text{SUSY}}^2$) as

$$v_u(Q) = \frac{v_u}{\sqrt{Z_{H_u}}}, \quad v_d(Q) = \frac{v_d}{\sqrt{Z_{H_d}}}, \quad s(Q) = \frac{s}{\sqrt{Z_S}}, \quad (30)$$

where Z_i , with $i = H_u, H_d, S$, are the wave function renormalisation constants. These constants multiply the kinetic terms in the effective action and their explicit forms are given in Appendix B. The elements of the Higgs mass matrix, therefore, have to be rescaled by appropriate powers of these renormalization constants as

$$\mathcal{M}'^2_{H,ij} = \mathcal{M}^2_{H,ij} / \sqrt{Z_i Z_j}. \quad (31)$$

This rescaling then takes care of further contributions of the order $g^2 h_{t,b}^2$ to the Higgs mass matrix.

2.3 Physical Higgs boson masses

To obtain the physical mass eigenstates the 6×6 Higgs mass matrix \mathcal{M}'^2_H can be diagonalised using the orthogonal matrix O as

$$(H_1, H_2, H_3, H_4, H_5, H_6)_a^T = O_{ai} (H_{dR}, H_{uR}, S_R, H_{dI}, H_{uI}, S_I)_i^T. \quad (32)$$

However, one of the resulting states corresponds to a massless Nambu-Goldstone (NG) mode, G . In order to isolate this NG mode, a β rotation of \mathcal{M}'^2_P is carried out, before the above diagonalisation, as

$$\begin{pmatrix} H_{dI} \\ H_{uI} \\ S_I \end{pmatrix} = \begin{pmatrix} \cos \beta & \sin \beta & 0 \\ -\sin \beta & \cos \beta & 0 \\ 0 & 0 & 1 \end{pmatrix} \begin{pmatrix} G \\ H_I \\ S_I \end{pmatrix}. \quad (33)$$

In the new basis, $\mathbf{h}^T \equiv (H_{dR}, H_{uR}, S_R, H_I, S_I)$, after dropping the NG mode, the tree level pseudoscalar block in eq. (10) gets replaced by

$$\mathcal{M}^2_{P_\beta} = \begin{pmatrix} (R_\lambda + \mathcal{R}s/2) \frac{v^2 s}{v_d v_u} & (R_\lambda - \mathcal{R}s)v \\ (R_\lambda - \mathcal{R}s)v & R_\lambda \frac{v_d v_u}{s} + 2\mathcal{R}v_d v_u - 3R_\kappa s \end{pmatrix}, \quad (34)$$

where $v = \sqrt{v_u^2 + v_d^2}$, and the off-diagonal CP-mixing block by

$$\mathcal{M}^2_{SP_\beta} = \begin{pmatrix} 0 & -\frac{3}{2}\mathcal{I}sv_u \\ 0 & -\frac{3}{2}\mathcal{I}sv_d \\ \frac{1}{2}\mathcal{I}sv & -2\mathcal{I}v_u v_d \end{pmatrix}. \quad (35)$$

The radiatively corrected Higgs mass matrix in the new basis can be obtained by similarly β -rotating the mass matrix given in eq. (31) as

$$\mathcal{M}'^2_h = (\mathcal{M}'^2_H)_\beta. \quad (36)$$

The effective potential masses of the neutral Higgs bosons are then obtained by diagonalising the above 5×5 mass matrix as $O'^T \mathcal{M}'^2_h O' = \text{diag}(m_{h_1}^2, m_{h_2}^2, m_{h_3}^2, m_{h_4}^2, m_{h_5}^2)$, such that

$$m_{h_1}^2 \leq m_{h_2}^2 \leq m_{h_3}^2 \leq m_{h_4}^2 \leq m_{h_5}^2. \quad (37)$$

For Higgs boson pole masses the approximate expression obtained in [38] can be extrapolated to the cNMSSM as

$$m_{h_i}^{\text{pole } 2} = m_{h_i}^2 - \frac{3h_t^2}{16\pi^2} \left[(m_{h_i}^2 - 4m_t^2) O_{i2}^2 + m_{h_i}^2 O_{i5}^2 \right] B(m_{h_i}^2, m_t^2) - \frac{3h_b^2}{16\pi^2} \left[m_{h_i}^2 (O_{i1}^2 + O_{i4}^2) \ln \left(\frac{m_t^2}{m_b^2} \right) + ((m_{h_i}^2 - 4m_b^2) O_{i1}^2 + m_{h_i}^2 O_{i4}^2) B(m_{h_i}^2, m_b^2) \right], \quad (38)$$

where the function $B(M^2, m^2)$ is defined as

$$B(M^2, m^2) = \begin{cases} 2 - \sqrt{1 - \frac{4m^2}{M^2}} \ln \left(\frac{1 + \sqrt{1 - \frac{4m^2}{M^2}}}{1 - \sqrt{1 - \frac{4m^2}{M^2}}} \right) : & M^2 > 4m^2, \\ 2 - 2\sqrt{\frac{4m^2}{M^2} - 1} \arctan \left(\sqrt{\frac{M^2}{4m^2 - M^2}} \right) : & M^2 < 4m^2. \end{cases} \quad (39)$$

In case of the charged Higgs states, a β rotation is also carried out for isolating the NG modes. The corrections to the charged Higgs boson mass, of the order $h_{t,b}^4$ and those induced by chargino/neutralino, gauge boson and slepton loops give rise to some additional terms on top of the shifts of A_λ described earlier. After including these corrections and β -rotating, the mass of the physical charged Higgs boson is given as

$$\begin{aligned} \mathcal{M}'_\pm{}^2 &= \left[(R_\lambda + \mathcal{R}s/2)s + v_u(Q)v_d(Q) \left(\frac{g_2^2}{2} - |\lambda|^2 \right) \right] \left(\frac{v_u(Q)}{Z_{H_d}v_d(Q)} + \frac{v_d(Q)}{Z_{H_u}v_u(Q)} \right) \\ &+ \frac{v_u^2(Q) + v_d^2(Q)}{16\pi^2} \left[6h_t^2 h_b^2 \ln \left(\frac{M_{\text{SUSY}}^2}{m_t^2} \right) - \frac{3}{4} g_2^4 \ln \left(\frac{M_{\text{SUSY}}^2}{m_l^2} \right) \right. \\ &\left. + \frac{7g_1^2 g_2^2 - g_2^4}{4} \ln \left(\frac{M_{\text{SUSY}}^2}{m_Z^2} \right) + 2(g_1^2 g_2^2 - g_2^4) L_{M_2\mu} \right], \end{aligned} \quad (40)$$

where the rescaling by the wave function normalisation constants has been taken care of. The pole mass of the charged Higgs boson is then obtained as

$$\begin{aligned} m_{h^\pm}^{\text{pole } 2} &= \mathcal{M}'_\pm{}^2 + \frac{3}{16\pi^2} \left\{ (h_t^2 \cos^2 \beta + h_b^2 \sin^2 \beta) \left(\mathcal{M}'_\pm{}^2 \left[\left(1 - \frac{m_t^2}{\mathcal{M}'_\pm{}^2} \right) \ln \left| \frac{\mathcal{M}'_\pm{}^2 - m_t^2}{m_t^2} \right| - 2 \right] \right. \right. \\ &+ (m_t^2 + m_b^2) \left[\left(1 - \frac{m_t^2}{\mathcal{M}'_\pm{}^2} \right) \ln \left| \frac{m_t^2}{\mathcal{M}'_\pm{}^2 - m_t^2} \right| + 1 \right] \Bigg) \\ &\left. + \frac{4m_t^2 m_b^2}{v^2} \left[\left(1 - \frac{m_t^2}{\mathcal{M}'_\pm{}^2} \right) \ln \left| \frac{m_t^2}{\mathcal{M}'_\pm{}^2 - m_t^2} \right| + 1 \right] \right\}. \end{aligned} \quad (41)$$

3 Trilinear Higgs boson self-interactions

The complete NMSSM Lagrangian contains the interaction terms of the Higgs bosons with the fermions, scalars and vector bosons as well as with each other, from which the corresponding couplings can be obtained. In table 1 we summarize various Higgs boson couplings which will be used in the expressions for neutral Higgs boson decay widths in the next section. The analytical formulae for these couplings in the cNMSSM, with the exception of the Higgs boson self-couplings,

can be found in [52] and [55]. The couplings between three neutral Higgs bosons, obtained from the potential in eq. (3), are given as

$$\begin{aligned}
g_{h_a h_b h_c} = & \frac{g^2}{4} \left(v_u (\Pi_{abc}^{111} - \Pi_{abc}^{122} + \Pi_{abc}^{144} - \Pi_{abc}^{155}) + v_d (\Pi_{abc}^{222} - \Pi_{abc}^{211} + \Pi_{abc}^{255} - \Pi_{abc}^{244}) \right) \\
& + \frac{\lambda^2}{2} \left(v_u (\Pi_{abc}^{122} + \Pi_{abc}^{133} + \Pi_{abc}^{155} + \Pi_{abc}^{166}) + v_d (\Pi_{abc}^{211} + \Pi_{abc}^{233} + \Pi_{abc}^{244} + \Pi_{abc}^{266}) \right. \\
& + s (\Pi_{abc}^{311} + \Pi_{abc}^{322} + \Pi_{abc}^{344} + \Pi_{abc}^{355}) \left. \right) + \kappa^2 s \left(\Pi_{abc}^{333} + \Pi_{abc}^{366} \right) \\
& - R_\lambda \left(\Pi_{abc}^{123} - \Pi_{abc}^{453} - \Pi_{abc}^{426} - \Pi_{abc}^{156} \right) + R_\kappa \left(\Pi_{abc}^{333} - 3\Pi_{abc}^{366} \right) \\
& - \frac{\mathcal{R}}{2} \left(v_u (\Pi_{abc}^{233} - \Pi_{abc}^{266} + 2\Pi_{abc}^{536}) + v_d (\Pi_{abc}^{133} - \Pi_{abc}^{166} + \Pi_{abc}^{436}) \right. \\
& + 2s (\Pi_{abc}^{123} - \Pi_{abc}^{345} + \Pi_{abc}^{156} + \Pi_{abc}^{426}) \left. \right) \\
& - \frac{\mathcal{I}}{2} \left(v_u (\Pi_{abc}^{566} - \Pi_{abc}^{533} + 2\Pi_{abc}^{236}) + v_d (\Pi_{abc}^{466} - \Pi_{abc}^{433} + \Pi_{abc}^{136}) \right. \\
& + s (3\Pi_{abc}^{126} - 3\Pi_{abc}^{456} - \Pi_{abc}^{135} - \Pi_{abc}^{423}) + 3 \frac{v_d v_u}{s} (\Pi_{abc}^{666} - \Pi_{abc}^{336}) \left. \right), \tag{42}
\end{aligned}$$

where

$$\Pi_{abc}^{ijk} = O_{ai} O_{bj} O_{ck} + O_{ai} O_{cj} O_{bk} + O_{bi} O_{aj} O_{ck} + O_{bi} O_{cj} O_{ak} + O_{ci} O_{aj} O_{bk} + O_{ci} O_{bj} O_{ak}, \tag{43}$$

with O_{xy} being the elements of the Higgs mixing matrix defined in eq. (32). The couplings of the neutral Higgs bosons to a pair of charged Higgs bosons are similarly given as

$$\begin{aligned}
g_{h_a h^+ h^-} = & \frac{g_1^2}{8} \left(v_u (\Pi_{abc}^{111} - \Pi_{abc}^{122}) + v_d (\Pi_{abc}^{222} - \Pi_{abc}^{211}) \right) \\
& + \frac{g_2^2}{8} \left(v_u (\Pi_{abc}^{111} + \Pi_{abc}^{122} + 2\Pi_{abc}^{212}) + v_d (\Pi_{abc}^{222} + \Pi_{abc}^{211} + 2\Pi_{abc}^{112}) \right) \\
& + \frac{\lambda^2}{2} \left(s (\Pi_{abc}^{311} + \Pi_{abc}^{322}) - v_u \Pi_{abc}^{212} - v_d \Pi_{abc}^{112} \right) \\
& + \mathcal{R} s \Pi_{abc}^{312} + R_\lambda \Pi_{abc}^{312} + \frac{3}{2} \mathcal{I} s \Pi_{abc}^{612}, \tag{44}
\end{aligned}$$

where

$$\Pi_{abc}^{ijk} = 2O_{ai} C_j C_k \text{ with } C_1 = \cos \beta, C_2 = \sin \beta. \tag{45}$$

4 Neutral Higgs boson decays

In this section, we present the analytical expressions for the decay widths of the cNMSSM Higgs bosons into pairs of fermions, massive gauge bosons, sfermions, photons, gluons and lighter Higgs bosons as well as into a lighter Higgs and massive gauge boson pair. These expressions have mostly been adopted from [56] and follow the notation therein. For the decay modes involving an off-mass-shell gauge boson, three-body decays are described following [57].

- $h \rightarrow f f'$

<i>fermion pair</i>	$g_{h_a \bar{f} f}^S$	$g_{h_a \bar{f} f}^P$
$d\bar{d}/l^+l^-$	$O_{a1}/\cos\beta$	$-O_{a4}/\cos\beta$
$u\bar{u}$	$O_{a2}/\sin\beta$	$-O_{a5}/\sin\beta$
$\tilde{\chi}_j^0 \tilde{\chi}_k^0$	$g_{h_a \tilde{\chi}_j^0 \tilde{\chi}_k^0}^S$	$g_{h_a \tilde{\chi}_j^0 \tilde{\chi}_k^0}^P$
$\tilde{\chi}_j^- \tilde{\chi}_k^+$	$g_{h_a \tilde{\chi}_j^- \tilde{\chi}_k^-}^S$	$g_{h_a \tilde{\chi}_j^+ \tilde{\chi}_k^-}^P$
<i>sfermions</i>	$g_{h_a \tilde{f} b \tilde{f}_c^*}$	
<i>gauge bosons</i>	$g_{h_a VV}$	
<i>Higgs + Z boson</i>	$g_{h_a h_b Z}$	
<i>neutral Higgs bosons</i>	$g_{h_a h_b h_c}$	
<i>charged Higgs bosons</i>	$g_{h_a h^+ h^-}$	

Table 1: The couplings of the NMSSM Higgs boson h_a to particles and sparticles at the tree level. $g_{h_a \bar{f} f}^S$ and $g_{h_a \bar{f} f}^P$ refer to vector and axial vector couplings of the fermions, respectively. O_{ai} are the elements of the Higgs mixing matrix defined in Sect. 2.3.

The decay width of a Higgs boson into two fermions is given as

$$\begin{aligned}
\Gamma(h_a \rightarrow f f') &= N_C \frac{G_F M_{h_a} \lambda^{1/2}(1, \kappa_{af}, \kappa_{af'})}{4\sqrt{2}\pi} \bar{m}_q^2(m_{h_a}) \Gamma_M K_a^f \\
&\times [(1 - \kappa_{af} - \kappa_{af'}) (|g_{h_a f f'}^S|^2 + |g_{h_a f f'}^P|^2) \\
&- 2\sqrt{\kappa_{af} \kappa_{af'}} (|g_{h_a f f'}^S|^2 - |g_{h_a f f'}^P|^2)] ,
\end{aligned} \tag{46}$$

where $G_F/\sqrt{2} = g_2^2/8m_W^2$, with m_W being the W boson mass, $\kappa_{af^{(\prime)}}$ $\equiv m_{f^{(\prime)}}^2/m_{h_a}^2$, $\lambda(1, x, y) \equiv (1 - x - y)^2 - 4xy$ and the couplings $g_{h_a f f'}^S$ and $g_{h_a f f'}^P$ have been defined in the previous section. The colour factor N_C is equal to 3 for quarks and to 1 for leptons, charginos, and neutralinos. $\Gamma_M = \left(\frac{4}{1+\delta_{bc}}\right)$ for Majorana fermions such as (s)neutrinos, neutralinos and charginos, with $\delta_{bc} = 1$ when they are identical, while for Dirac fermions $\Gamma_M = 1$. For $h_a \rightarrow q\bar{q}$ the leading-order QCD corrections are taken into account with the enhancement factor $K_a^q = 1 + 5.67 \frac{\alpha_s(m_{h_a}^2)}{\pi}$. For leptons, neutralinos and charginos, $K_a^f = 1$.

• $h \rightarrow VV$

The decay width into two massive gauge bosons is given as

$$\Gamma(h_a \rightarrow VV) = \delta_V \frac{G_F g_{h_a VV}^2 m_{h_a}^3}{16\sqrt{2}\pi} \beta_{iV} (1 - 4\kappa_{aV} + 12\kappa_{aV}^2), \tag{47}$$

where $\kappa_{aV} = m_V^2/m_{h_a}^2$, $\beta_{aV} = \sqrt{1 - 4\kappa_{aV}}$, $\delta_W = 2$ and $\delta_Z = m_W^4/(\cos\theta_W m_Z)^4 = 1$. Below VV threshold, when one of the gauge bosons is off-mass-shell, the three-body decay width of a Higgs boson is given as

$$\Gamma(h_a \rightarrow VV^*) = \delta'_V \frac{3G_F g_{h_a VV}^2 m_{h_a} m_V^4}{16\sqrt{2}\pi} R(\kappa_{aV}), \tag{48}$$

where $\delta'_W = 2$, $\delta'_Z = 7/12 - 10\sin^2\theta_W/9 + 40\sin^4\theta_W/27$ and

$$R(x) = 3 \frac{1 - 8x + 20x^2}{\sqrt{4x - 1}} \arccos\left(\frac{3x - 1}{2x^{3/2}}\right) - \frac{1 - x}{2x} (2 - 13x + 47x^2) - \frac{3}{2} (1 - 6x + 4x^2) \log x. \tag{49}$$

• $h_a \rightarrow h_b h_c, \tilde{f}_b \tilde{f}_c^*$

The decay width of a Higgs boson into two scalar particles, including sfermions and lighter Higgs bosons, is written as

$$\Gamma(h_a \rightarrow h_b h_c, \tilde{f}_b \tilde{f}_c^*) = \frac{N_F |\mathcal{G}|^2}{16\pi m_{h_a}} \lambda^{1/2}(1, \kappa_{ab}, \kappa_{ac}), \quad (50)$$

where $(N_F, \mathcal{G}) = (1/(1 + \delta_{bc}), g_{h_a h_b h_c})$, $(N_C, g_{h_a \tilde{f}_b \tilde{f}_c^*})$ and $\kappa_{ai} = m_{h_i, \tilde{f}_i}^2 / m_{h_a}^2$.

• $h_a \rightarrow h_b Z$

The decay width of a Higgs boson into a lighter Higgs and Z boson pair is given as

$$\Gamma(h_a \rightarrow h_b Z) = g_{h_a h_b Z}^2 \frac{G_F m_Z^4}{8\sqrt{2}\pi m_{h_a}} \sqrt{\lambda'(m_{h_b}^2, m_Z^2; m_{h_a}^2)} \lambda'(m_{h_b}^2, m_{h_a}^2; m_Z^2), \quad (51)$$

where the function $\lambda'(x, y; z) = (1 - x/z - y/z)^2 - 4xy/z^2$. Below the threshold for the above process, the three-body decay width is given as

$$\Gamma(h_a \rightarrow h_b Z^*) = g_{h_a h_b Z}^2 \delta'_Z \frac{9G_F^2 m_Z^4 m_{h_a}}{8\pi^3} G_{h_b Z}, \quad (52)$$

where the generic functions G_{ij} can be written as

$$G_{ij} = \frac{1}{4} \left\{ 2(-1 + \kappa_j - \kappa_i) \sqrt{\lambda_{ij}} \left[\frac{\pi}{2} + \arctan \left(\frac{\kappa_j(1 - \kappa_j + \kappa_i) - \lambda_{ij}}{(1 - \kappa_i) \sqrt{\lambda_{ij}}} \right) \right] \right. \quad (53)$$

$$\left. + (\lambda_{ij} - 2\kappa_i) \log \kappa_i + \frac{1}{3}(1 - \kappa_i) \left[5(1 + \kappa_i) - 4\kappa_j - \frac{2}{\kappa_j} \lambda_{ij} \right] \right\}, \quad (54)$$

using the parameters

$$\lambda_{ij} = -1 + 2\kappa_i + 2\kappa_j - (\kappa_i - \kappa_j)^2; \quad \kappa_i = \frac{m_i^2}{m_{h_a}^2}. \quad (55)$$

• $h \rightarrow Z\gamma$

The decay width of a Higgs boson into a Z boson and photon pair is given by

$$\Gamma(h_a \rightarrow Z\gamma) = \frac{G_F m_W^2 \alpha^2 m_{h_a}^3}{64\pi^3} (1 - \kappa_{aZ})^3 \left[|S_a^{Z\gamma}(m_{h_a})|^2 + |P_a^{Z\gamma}(m_{h_a})|^2 \right]. \quad (56)$$

In the above expression the scalar and pseudoscalar form factors, retaining only the dominant loop contributions, which include those from t and b quarks, W^\pm and H^\pm , are given by

$$\begin{aligned} S_a^{Z\gamma}(m_{h_a}) &= \sum_{f=b,t} g_{h_a \bar{f} f}^S F'_{sf}(\tau_{af}, \lambda_f) + g_{h_a VV} F'_1(\tau_{aW}, \lambda_W) \\ &\quad + \frac{g_{h_a h^+ h^-}}{2\sqrt{2}G_F m_{h^\pm}^2} F'_0(\tau_{ah^\pm}, \lambda_{h^\pm}), \\ P_a^{Z\gamma}(m_{h_a}) &= \sum_{f=b,t} g_{h_a \bar{f} f}^P F'_{pf}(\tau_{af}, \lambda_f), \end{aligned} \quad (57)$$

where $\tau_{ax} = 4m_x^2/m_{h_a}^2$ and $\lambda_x = 4m_x^2/m_Z^2$. The form factors F'_{sf} , F'_{pf} , F'_0 and F'_1 are given as

$$\begin{aligned}
F'_{sf}(\tau, \lambda) &= 6 \frac{Q_f(I_{3f} - 2Q_f \sin^2 \theta_W)}{\cos \theta_W} [I_1(\tau, \lambda) - I_2(\tau, \lambda)] , \\
F'_{pf}(\tau, \lambda) &= 12 \frac{Q_f(I_{3f} - 2Q_f \sin^2 \theta_W)}{\cos \theta_W} I_2(\tau, \lambda) , \\
F'_0(\tau, \lambda) &= \frac{\cos 2\theta_W}{\cos \theta_W} I_1(\tau, \lambda) , \\
F'_1(\tau, \lambda) &= \cos \theta_W \left\{ 4(3 - \tan^2 \theta_W) I_2(\tau, \lambda) \right. \\
&\quad \left. + \left[\left(1 + \frac{2}{\tau}\right) \tan^2 \theta_W - \left(5 + \frac{2}{\tau}\right) \right] I_1(\tau, \lambda) \right\} ,
\end{aligned} \tag{58}$$

where Q_f is the electric charge of the fermion f and I_{3f} is the third component of its isospin. The functions $I_{1,2}$ are defined as

$$I_1(\tau, \lambda) = \frac{\tau\lambda}{2(\tau - \lambda)} + \frac{\tau^2\lambda^2}{2(\tau - \lambda)^2} [f(\tau) - f(\lambda)] + \frac{\tau^2\lambda}{(\tau - \lambda)^2} [g(\tau) - g(\lambda)] , \tag{59}$$

$$I_2(\tau, \lambda) = -\frac{\tau\lambda}{2(\tau - \lambda)} [f(\tau) - f(\lambda)] , \tag{60}$$

with

$$g(\tau) = \begin{cases} \sqrt{\tau - 1} \arcsin \frac{1}{\sqrt{\tau}} & \tau \geq 1 \\ \frac{\sqrt{1 - \tau}}{2} \left[\log \frac{1 + \sqrt{1 - \tau}}{1 - \sqrt{1 - \tau}} - i\pi \right] & \tau < 1 . \end{cases} \tag{61}$$

• $h \rightarrow \gamma\gamma$

The decay width into two photons is given as

$$\Gamma(h_a \rightarrow \gamma\gamma) = \frac{G_F \alpha^2 m_{h_a}^3}{128 \sqrt{2} \pi^3} \left[|S_a^\gamma(m_{h_a})|^2 + |P_a^\gamma(m_{h_a})|^2 \right] , \tag{62}$$

where α is the fine-structure constant. The scalar and pseudoscalar form factors, retaining only the loop contributions from W^\pm , H^\pm and the dominant ones from (s)fermions, are given by

$$\begin{aligned}
S_a^\gamma(m_{h_a}) &= 2 \sum_{f=b,t,\tilde{\chi}_1^\pm,\tilde{\chi}_2^\pm} N_C Q_f^2 g_{h_a \bar{f} f}^S F_{sf}(\tau_{af}) \\
&\quad + \sum_{\tilde{f}_j=\tilde{t}_1,\tilde{t}_2,\tilde{b}_1,\tilde{b}_2,\tilde{\tau}_1,\tilde{\tau}_2} N_C Q_f^2 \frac{g_{H_i \tilde{f}_j^* \tilde{f}_j}}{2\sqrt{2} G_F m_{\tilde{f}_j}^2} F_0(\tau_{a\tilde{f}_j}) \\
&\quad + g_{h_a VV} F_1(\tau_{aW}) + \frac{g_{h_a h^+ h^-}}{2\sqrt{2} G_F m_{h^\pm}^2} F_0(\tau_{ah^\pm}) , \\
P_a^\gamma(m_{h_a}) &= 2 \sum_{f=b,t,\tilde{\chi}_1^\pm,\tilde{\chi}_2^\pm} N_C Q_f^2 g_{h_a \bar{f} f}^P F_{pf}(\tau_{af}) .
\end{aligned} \tag{63}$$

The form factors F_{sf} , F_{pf} , F_0 and F_1 in the above equations are given as

$$\begin{aligned}
F_{sf}(\tau) &= \tau [1 + (1 - \tau)f(\tau)] , \quad F_{pf}(\tau) = \tau f(\tau) , \\
F_0(\tau) &= -\tau [1 - \tau f(\tau)] , \quad F_1(\tau) = -[2 + 3\tau + 3\tau(2 - \tau)f(\tau)] ,
\end{aligned} \tag{64}$$

in terms of the scaling function $f(\tau)$ written as

$$f(\tau) = \begin{cases} \arcsin^2\left(\frac{1}{\sqrt{\tau}}\right) : & \tau \geq 1, \\ -\frac{1}{4} \left[\ln\left(\frac{1+\sqrt{1-\tau}}{1-\sqrt{1-\tau}}\right) - i\pi \right]^2 : & \tau < 1. \end{cases} \quad (65)$$

• $h \rightarrow gg$

The decay width of a Higgs boson into two gluons is given by

$$\Gamma(h_a \rightarrow gg) = \frac{G_F \alpha_S^2 m_{h_a}^3}{16\sqrt{2}\pi^3} \left[K_S^g |S_a^g(m_{h_a})|^2 + K_P^g |P_a^g(m_{h_a})|^2 \right], \quad (66)$$

where α_S is the strong coupling constant and the scalar and pseudoscalar form factors, retaining only the contributions from third-generation (s)quarks, are given by

$$\begin{aligned} S_a^g(m_{h_a}) &= \sum_{f=b,t} g_{haf\bar{f}}^S F_{sf}(\tau_{af}) + \sum_{\tilde{f}_j=\tilde{t}_1,\tilde{t}_2,\tilde{b}_1,\tilde{b}_2} \frac{g_{h_a\tilde{f}_j^*\tilde{f}_j}}{4\sqrt{2}G_F m_{\tilde{f}_j}^2} F_0(\tau_{a\tilde{f}_j}), \\ P_a^g(m_{h_a}) &= \sum_{f=b,t} g_{haf\bar{f}}^P F_{pf}(\tau_{af}), \end{aligned} \quad (67)$$

with functions F_{sf} , F_{pf} and F_0 , being the same as for the $\gamma\gamma$ mode above. $K_{S,P}^g$ in eq. (66) are QCD loop enhancement factors that include the leading-order QCD corrections. In the heavy-quark limit, the factors $K_{H,A}^g$ are given by [58]

$$\begin{aligned} K_S^g &= 1 + \frac{\alpha_S(M_{H_i}^2)}{\pi} \left(\frac{95}{4} - \frac{7}{6} N_F \right), \\ K_P^g &= 1 + \frac{\alpha_S(M_{H_i}^2)}{\pi} \left(\frac{97}{4} - \frac{7}{6} N_F \right), \end{aligned} \quad (68)$$

where N_F is the number of quark flavours lighter than the h_a boson.

5 Novel heavy Higgs boson decays into SM-like 125 GeV states

In this section we discuss a very interesting cNMSSM scenario which, if probed at the LHC, could provide an indication of not only the existence of CP violation in the Higgs sector but also of a non-minimal nature of SUSY. For a numerical analysis of this scenario, we use a fortran program (available on request) in which the Higgs mass matrix and the expressions for decay widths described earlier have been implemented along with other SUSY mass matrices (given in Appendix A). This program computes the Higgs boson masses and BRs as well as the SUSY mass spectrum for a given set of the cNMSSM input parameters defined at M_{SUSY} . The package also tests the output of a given point in the cNMSSM parameter space against the constraints from the direct searches of the SM (and SUSY) Higgs boson(s) as well as third generation squark, stau and light chargino at LEP. Although no limits from b -physics, LHC SUSY searches or from relic density measurements have so far been implemented in the package, in our current analysis we confine ourselves to

points from among those which have been found to best comply with such constraints (see, e.g., [40, 41, 59, 60, 61, 62, 63, 64, 65, 66]).

In the experimental searches the magnitude of the signal is typically characterized by the ‘signal strength’, $\mu(X) \equiv \sigma_{\text{obs}}(X)/\sigma_{h_{\text{SM}}}(X)$, where h_{SM} implies a SM Higgs boson with mass equal to the measured one of the observed boson decaying via a given channel X . The theoretical counterpart of this quantity, sometimes referred to as the *reduced cross section*, for a Higgs boson, h_i , produced in the dominant gluon fusion mode is given as

$$\mu_{h_i}(X) = \frac{\sigma(gg \rightarrow h_i)}{\sigma(gg \rightarrow h_{\text{SM}})} \times \frac{\text{BR}(h_i \rightarrow X)}{\text{BR}(h_{\text{SM}} \rightarrow X)}. \quad (69)$$

To a good approximation, the ratio of the production cross sections σ of h_i and h_{SM} in the above expression can be substituted by the ratio of their respective decay widths into two gluons. We, therefore, redefine the reduced cross section as

$$R_{h_i}(X) \equiv \frac{\Gamma(h_i \rightarrow gg)}{\Gamma(h_{\text{SM}} \rightarrow gg)} \times \frac{\text{BR}(h_i \rightarrow X)}{\text{BR}(h_{\text{SM}} \rightarrow X)}, \quad (70)$$

for our analysis below.

As noted earlier, the presence of non-zero CPV phases in the Higgs sector of the NMSSM can result in some unique scenarios which are not possible when CP is conserved. In particular, an decrease in the mass of a given Higgs boson with a variation in CPV phases can result in the kinematical opening of new decay channels. Conversely, a gradual decrease in the Higgs boson mass can result in the closing of a particular decay channel beyond a certain value of a given CPV phase, thereby causing a notable reduction in its total width and a deviation in its BRs from the CPC case. Indeed such deviations were observed for a ~ 125 GeV SM-like Higgs boson in [43], owing sometimes to the contribution of the CPV phases to the gaugino masses also besides the Higgs boson mass itself. Another crucial possibility arises due to the fact that the Higgs mass eigenstates do not carry a definite CP assignment for non-zero CPV phases. Hence, couplings between pseudoscalar and scalar states which are forbidden in the CPC limit become possible upon the introduction of such phases, resulting in some ‘unconventional’ Higgs boson decays.

In the NMSSM, in analogy with the decoupling regime of the MSSM, when one of the CP-even Higgs bosons is required to have exactly SM-like couplings and a mass around 125 GeV the other doublet-like scalar and pseudoscalar Higgs bosons are typically very heavy, $\gtrsim 500$ GeV. In this case a correlation exists between the masses of the light doublet-like and the singlet-like scalar Higgs bosons such that the latter is either lighter than the former, in a small portion of the parameter space, or decoupled like the other heavy doublet-like Higgs bosons. On the other hand, the mass of the singlet-like pseudoscalar, typically a_1 , approximated at the leading order (for large $\tan\beta$) by

$$m_{a_1}^2 \simeq -\kappa s A_\kappa, \quad (71)$$

can vary much more freely depending on the size of the parameter A_κ , with marginal affect on the masses of the other Higgs bosons. It is thus possible for a_1 to have a mass close to twice that of the SM-like Higgs boson. Note also the fact that the partial decay width of a given Higgs boson, h_a , into two lighter Higgs bosons, given in eq. (51), is inversely proportional to m_{h_a} . Hence, when CPV phases are turned on, the decay amplitude of a (now CP-indefinite) ~ 250 GeV Higgs boson into a pair of SM-like Higgs bosons can become sizable.

In the following we will further discuss the representative points of three benchmark cNMSSM parameter space cases wherein not only a SM-like ~ 125 GeV Higgs boson but also the above mentioned ~ 250 GeV Higgs boson can be obtained. We will analyse in detail the impact of

variation in the CPV phase ϕ_κ ¹ on the properties of the relevant Higgs bosons for these points. We should indicate here that the chosen points exhibiting our scenario of interest are indeed not isolated ones and dedicated scans of their neighbourhoods in the model parameter space should reveal many more similar points. However, such scans are beyond the scope of this article since our aim here is to highlight some specific characteristics of the parameter regions yielding our representative points, rather than to map out their sizes. For convenience, we shall refer to the singlet-like pseudoscalar(-like) Higgs boson generically as h_p , to the ~ 125 GeV SM-like Higgs boson as h_d and to the other singlet-dominated scalar(-like) boson as h_s henceforth.

In principle, since the coupling of h_p to a pair of h_d is only induced by CPV phases one can expect the corresponding partial decay width and BR to be minimal. However, as noted above, the fact that the mass of h_p lies much closer to the $h_d h_d$ production threshold than that of the heavy doublet-like Higgs bosons is crucial and provides a unique possibility in the context of Higgs boson phenomenology at the LHC. Therefore, for quantifying the magnitude of the process where h_p produced via gluon fusion decays into one or more h_d which subsequently decay in the channel X , we compute, following eq. (70), the auxiliary quantity

$$A_{di}^{h_p}(\gamma\gamma) \equiv \frac{\Gamma(h_p \rightarrow gg)}{\Gamma(h_{\text{SM}} \rightarrow gg)} \times \text{BR}(h_p \rightarrow h_d h_i) \times \frac{n_i \text{BR}(h_d \rightarrow \gamma\gamma)}{\text{BR}(h_{\text{SM}} \rightarrow \gamma\gamma)}, \quad (72)$$

where h_{SM} refers to a SM Higgs boson with the same mass as h_d . $i = d, s$ in the above equation, since the decay $h_p \rightarrow h_d h_s$ is also possible when $m_{h_s} < m_{h_p} - m_{h_d}$, and the constant n_i is thus equal to 2 for $h_i = h_d$ and to 1 for $h_i = h_s$. Evidently both $A_{dd}^{h_p}(\gamma\gamma)$ and $A_{ds}^{h_p}(\gamma\gamma)$ are by definition zero in the CPC limit. We stress here that the above expression gives only a crude estimate of di-photon production rate via this channel, since the incoming gluons will require a larger momentum fraction for producing the heavier h_p than for h_{SM} and thus their structure functions will differ. However, while a calculation of the actual total cross section for the process $h_p \rightarrow h_d h_i \rightarrow XX$ is needed for an accurate estimate of its significance at the LHC, the above expression provides a reasonably good approximation since h_p in our scenario of interest is not much heavier than h_d . Evidently then, such an auxiliary signal rate cannot be defined for the other, much heavier, Higgs bosons of the model.

Furthermore, in our analysis below we will compute $R_{h_d}(X)$, defined in eq. (70), for $X = \gamma\gamma, ZZ$ for each benchmark case as a measure of the deviation of h_d from SM-like properties. $R_{h_d}(X) = 1$ thus implies that h_d has an exactly SM-like signal strength in the channel X . As for the SUSY inputs, we will impose the mSUGRA-inspired unification conditions,

$$\begin{aligned} M_0 &\equiv M_{Q_3} = M_{U_3} = M_{D_3} = M_{L_3} = M_{E_3} = M_{\text{SUSY}}, \\ M_{1/2} &\equiv 2M_1 = M_2 = \frac{1}{3}M_3, \\ A_0 &\equiv A_t = A_b = A_\tau, \end{aligned}$$

where $M_{\tilde{Q}_3}^2$, $M_{\tilde{U}_3}^2$, $M_{\tilde{D}_3}^2$ and $M_{\tilde{L}_3}^2$, $M_{\tilde{E}_3}^2$ are the soft SUSY-breaking squared masses of the third generation squarks and sleptons, respectively. Finally, we will fix $\text{sign}[\cos(\phi_\lambda + \phi_{A_\lambda})] = \text{sign}[\cos(\phi_\kappa + \phi_{A_\kappa})] = +1$.

¹Since only the difference $\phi'_\lambda - \phi'_\kappa$ enters the Higgs mass matrix at the tree level, the variation in Higgs boson properties with varying ϕ'_κ is almost identical to that with varying ϕ'_λ , as was noted in [43]. However, since ϕ'_κ is virtually unconstrained by the measurements of fermionic EDMs [55, 53], we only vary this phase in our analysis. Also, since ϕ_{A_0} does not contribute directly to the Higgs-to-Higgs decay width, its relevance to our scenario under consideration is minimal.

Point	M_0	$M_{1/2}$	A_0	$\tan\beta$	λ	κ	μ_{eff}	A_λ	A_κ
P1	2500	1200	-6000	15	0.09	0.11	1000	600	-30
P2	2500	1000	-3600	20	0.043	0.013	200	200	-200
P3	1000	500	-2500	15	0.54	0.34	140	185	-200

Table 2: Values of the cNMSSM parameters corresponding to the three benchmark cases discussed in text. All dimensionful parameters are in units of GeV.

5.1 $h_1 = h_d$

We first discuss the case when the lightest Higgs state, h_1 , is SM-like while h_p is the second lightest of the five neutral Higgs states of the model, hence corresponding to h_2 . As a representative of this case we choose the point P1, given in table 2, in the cNMSSM parameter space. This point yields h_d around 125 GeV in the CPC limit, with almost exactly SM-like signal strengths in the $\gamma\gamma$ and ZZ channels, despite a non-vanishing λ and, hence, singlet component (such a NMSSM Higgs boson has been discussed in [67]). In panel (a) of figure 1 we show the auxiliary signal rate $A_{dd}^{h_p}(\gamma\gamma)$ as a function of ϕ_κ for P1. We see that $A_{dd}^{h_p}(\gamma\gamma)$ rises gradually and reaches a maximum value, ~ 0.1 , for $\phi_\kappa = 29^\circ$. Such a h_p can thus be responsible for up to 10% of the observed $\gamma\gamma$ excess besides that due to the direct production of h_d in the gluon fusion channel. The increase in $A_{dd}^{h_p}(\gamma\gamma)$ with ϕ_κ is a twofold consequence of the gradual increase in the gluonic width of h_p and an increase in its BR into h_d pair. The reason for the cutoff in the line is that beyond $\phi_\kappa = 29^\circ$ the minimization condition given in eq. (9) is not satisfied any more.

In panel (b) we show the signal strength of h_p , produced via gluon fusion, in the $\gamma\gamma$ decay channel. We note that although there is a considerable rise in $R_{h_p}(\gamma\gamma)$ with increasing amount of CP violation, it hardly exceeds per mil level for allowed values of ϕ_κ . This is due to the fact that h_p has a significantly reduced coupling to two photons compared to that of a SM Higgs boson with the same mass. In panel (c) are shown the dominant BRs of h_p against its mass, with ϕ_κ increasing from left to right. This plot demonstrates the main reason of large auxiliary signal rates of h_p for non-zero ϕ_κ , as observed above. We see that as soon as the process $h_p \rightarrow h_d h_d$ is allowed, it becomes one of the dominant decay modes of h_p , with BR reaching up to 0.25 (large-dotted red line). However, it is still not the most dominant decay mode due to the fact that h_p develops non-zero couplings also to gauge boson pairs. Therefore, the decay $h_p \rightarrow W^+ W^-$ (dashed violet line) has the highest BR for non-zero ϕ_κ , while the BR of h_p into ZZ (small-dotted green line) also lies close to that into $h_d h_d$. As a result, the decay modes $h_p \rightarrow b\bar{b}$ (solid cyan line) and $h_p \rightarrow \tau^+ \tau^-$ (dot-dashed blue line), which had the highest and second highest BRs, respectively, in the CPC limit, become very subdominant. Since there is a negligible increase in the mass of h_p with increasing ϕ_κ , all the above BRs remain almost constant over the entire allowed range of this phase.

Finally, in panel (d) we show the signal strengths of h_d in the $\gamma\gamma$ and ZZ channels (solid green line and dashed red line, respectively) plotted against its mass. With increasing ϕ_κ (again, from left to right) m_{h_d} falls slowly. It reaches ~ 124.7 GeV for $\phi_\kappa = 29^\circ$ which, taking into account the fact that there are considerable theoretical uncertainties in the model prediction, is still consistent with the mass measurements at the LHC [68, 69] (which in turn have non-negligible experimental errors). We see in the figure that $R_{h_d}(ZZ)$ and $R_{h_d}(\gamma\gamma)$ are both very SM-like in the CPC limit, with the former slightly higher than the latter. With increasing ϕ_κ both these rates show a very slow drop, identically to each other.

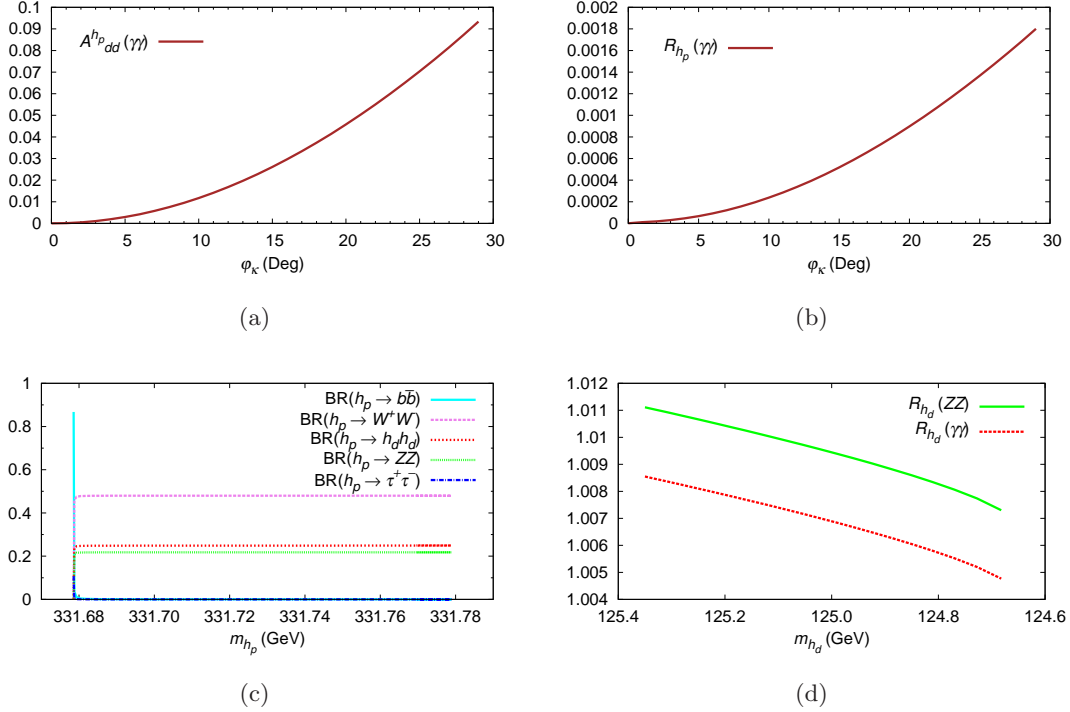


Figure 1: Case when $h_1 = h_d$ and $h_2 = h_p$. (a), (b) Signal rates $A_{dd}^{h_p}(\gamma\gamma)$ and $R_{h_p}(\gamma\gamma)$, respectively, as functions of ϕ_κ . (c) BRs of h_p into $b\bar{b}$ (solid cyan line), W^+W^- (dashed violet line), $h_d h_d$ (large-dotted red line), ZZ (small-dotted green line) and $\tau^+\tau^-$ (dot-dashed blue line) vs. m_{h_p} . (d) Signal strengths of h_d in the ZZ channel (solid green line) and in the $\gamma\gamma$ channel (dashed red line) vs. m_{h_d} .

5.2 $h_2 = h_d$

As stated in the Introduction, in the NMSSM the h_2 (the second lightest scalar in the CPC limit) can also be the ~ 125 GeV SM-like Higgs boson with the h_1 corresponding to h_s . Below we discuss two distinct cases, based on the compositions of h_1 and h_2 , in which this possibility is realised.

Small singlet-doublet mixing: For small λ , κ and μ_{eff} but intermediate-to-large $\tan\beta$, h_2 is still doublet-dominated and hence possesses very SM-like couplings to fermions and bosons. In this case, due to a smaller VeV s resulting from a lower value of μ_{eff} (recall that $\mu_{\text{eff}} = \lambda s$) compared to the case discussed above, the mass of the singlet-like scalar Higgs boson falls below that of h_d . In fact, owing to a highly dominant singlet component, m_{h_s} can reach very low values, ~ 40 GeV, before it violates the LEP limit on hZ production [70]. This effectively bounds m_{h_p} , which grows with increasing A_κ while m_{h_s} falls, from above. Thus it is extremely difficult for A_κ and, resultantly, m_{h_p} to become large enough to allow $h_p \rightarrow h_d h_d$ decay. However, thanks to a fairly light h_s , the decay $h_p \rightarrow h_d h_s$ is alternatively possible for non-zero ϕ_κ .

We choose the point P2, with its coordinates in the cNMSSM parameter space given in table 2, to demonstrate the effects of CPV on the phenomenology of h_p for this case. In panel (a) of figure 2 we show $A_{ds}^{h_p}(\gamma\gamma)$ against ϕ_κ for P2. We see in the figure that $A_{ds}^{h_p}(\gamma\gamma)$ grows steadily until $\phi_\kappa = 39^\circ$ after which it falls abruptly. The reason for this fall is the opening up of the $h_p \rightarrow \chi_1 \chi_1$ decay channel as we shall see below. Note that even the peak value of $A_{ds}^{h_p}(\gamma\gamma)$ for $\phi_\kappa = 39^\circ$ in this case

lies two orders of magnitude below the per mil level. It is, nevertheless, of the same order as the signal strength due to the $\gamma\gamma$ decay of h_p itself, as can be seen in panel (b). The cutoff at $\phi_\kappa = 76^\circ$ in the figures is due to the fact that beyond this value of the phase the slowly decreasing mass of h_s violates the above mentioned LEP limit.

The reason for the sudden drop in the various signal rates of h_p after $\phi_\kappa = 39^\circ$ becomes obvious from panel (c), where we show its dominant BRs plotted against m_{h_p} . In contrast with the first case above, even when $h_p \rightarrow h_d h_s$ decay channel (small-dotted red line) opens up for non-zero ϕ_κ , it remains very subdominant, with BR still smaller than that for the $h_p \rightarrow b\bar{b}$ mode (solid cyan line). We see in the figure that for small non-zero values of ϕ_κ the decay mode $h_p \rightarrow W^+ W^-$ (dashed violet line) is clearly the most dominant one, with BR as high as ~ 0.7 , while $h_p \rightarrow ZZ$ (large-dotted blue line) is the second most dominant mode. With increasing ϕ_κ (left to right) m_{h_p} falls negligibly, but just before it reaches 187.86 GeV, $\text{BR}(h_p \rightarrow \chi_1 \chi_1)$ (dot-dashed green line) suddenly shoots up. This is a consequence of the fact that m_{χ_1} also falls sharply as ϕ_κ is increased, so much so that for $\phi_\kappa > 39^\circ$ χ_1 becomes light enough to make the decay of h_p into its pair possible kinematically. Resultantly, beyond $\phi_\kappa = 39^\circ$ all the hitherto dominant decay modes, $h_p \rightarrow W^+ W^-$, $h_p \rightarrow ZZ$ and $h_p \rightarrow b\bar{b}$, grow increasingly subdominant while $\text{BR}(h_p \rightarrow h_d h_s)$ falls even further.

The above discussion of the behaviour of various BRs of h_p has an important implication, that χ_1 , at least for large values of ϕ_κ , is highly singlino-dominated. It should, therefore, be extremely difficult to probe at a direct detection experiment for dark matter, such as XENON [71]. In panel (d) we show the signal strengths of h_d against its mass for this case. m_{h_d} increases slowly with increasing ϕ_κ , conversely to P1, but the signal rates $R_{h_d}(ZZ)$ (solid green line) and $R_{h_d}(\gamma\gamma)$ (dashed red line) fall gradually, with the former always staying slightly above the latter. The two rates, however, never drop below 0.9 and hence always lie well within the experimental uncertainties around the measured central values at the LHC.

Large singlet-doublet mixing: It was noted in [40] that, for large λ and κ and small $\tan\beta$ and μ_{eff} , h_2 in the NMSSM (again, h_d here) can have a considerably enhanced $\gamma\gamma$ rate compared to h_{SM} , due mainly to the reduced coupling and consequently reduced $\text{BR}(h_d \rightarrow b\bar{b})$. This scenario, in which the h_1 (h_s here) has a mass lying just below m_{h_2} [41] and the lightest stop can have a mass significantly below 1 TeV [61], is sometimes referred to as the ‘natural NMSSM’ [72]. To discuss the impact of a light h_p on such a scenario in the cNMSSM we choose the point P3, given in table 2.

Unlike in the second case discussed above, in this case h_p can easily have a mass more than twice that of h_d , implying that its decay into $h_d h_d$ is possible simultaneously with that into $h_d h_s$, once CP is violated. In panels (a) and (b) of figure 3 we show $A_{dd}^{h_p}(\gamma\gamma)$ and $A_{ds}^{h_p}(\gamma\gamma)$, respectively, as functions of the phase ϕ_κ . We see that both these rates grow rapidly with increasing ϕ_κ , with $A_{ds}^{h_p}(\gamma\gamma)$ more so than $A_{dd}^{h_p}(\gamma\gamma)$, reaching ~ 0.5 for $\phi_\kappa = 5^\circ$. However, ϕ_κ is cutoff at this value due to the fact that both m_{h_d} and m_{h_s} fall rapidly with increasing ϕ_κ , as we shall see later. Thus for $\phi_\kappa > 5^\circ$ m_{h_d} becomes incompatible with the current LHC measurement of the Higgs boson mass, while the mass of h_s , which has a significant doublet component due to large mixing, violates the LEP bound mentioned earlier. Panel (c) shows that $R_{h_p}(\gamma\gamma)$ for this case also rises to percent level for $\phi_\kappa > 1^\circ$ and reaches a peak value very close to that of $A_{dd}^{h_p}(\gamma\gamma)$.

In panel (d) of figure 3 we show $\text{BR}(h_p \rightarrow h_d h_d)$ (solid green line) and $\text{BR}(h_p \rightarrow h_d h_s)$ (dashed red line) plotted against m_{h_p} , with ϕ_κ increasing from left to right. In contrast with the earlier cases, we see that neither of these two BRs reaches a value even as low as 0.1, even though they still yield significant $A^{h_p}(\gamma\gamma)$ rates as noted above. $\text{BR}(h_p \rightarrow h_d h_d)$ is dominant over $\text{BR}(h_p \rightarrow h_d h_s)$ for $\phi_\kappa \leq 3^\circ$, but becomes increasingly subdominant for larger ϕ_κ , owing to the fact that m_{h_s} starts falling faster than m_{h_d} . The reason for small BRs of h_p in these two decay modes becomes clear, once

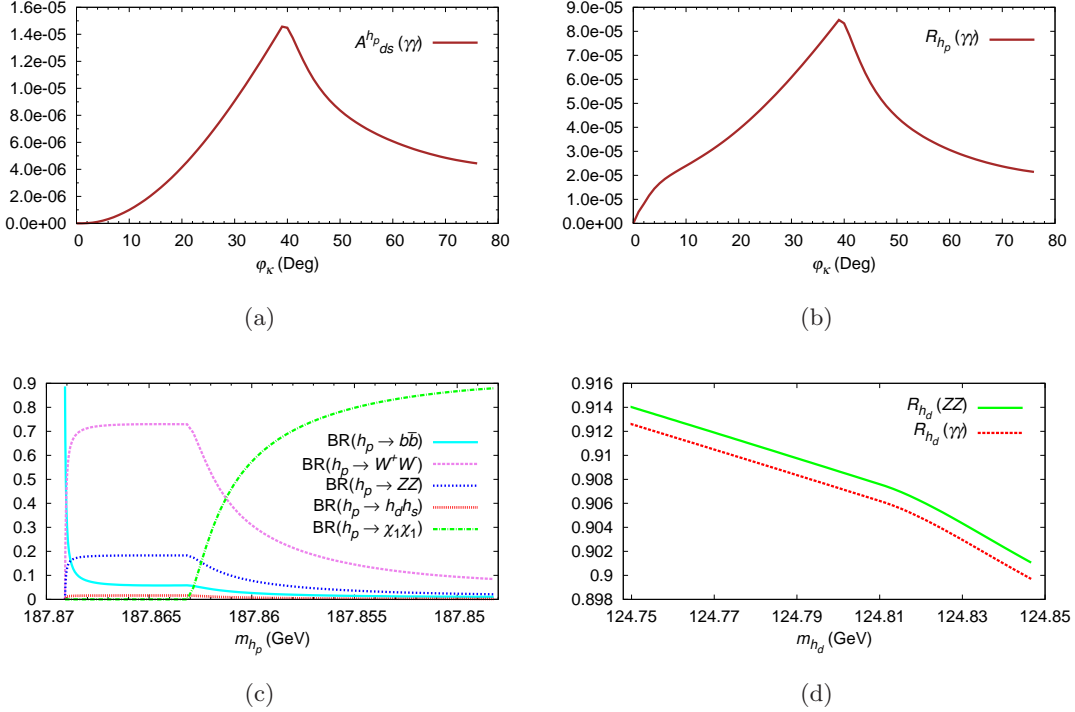


Figure 2: Case when $h_2 = h_d$ with small singlet-doublet mixing and $h_3 = h_p$. (a), (b) Signal rates $A_{ds}^{h_p}(\gamma\gamma)$ and $R_{h_p}(\gamma\gamma)$, respectively, as functions of ϕ_κ . (c) BRs of h_p into $b\bar{b}$ (solid cyan line), W^+W^- (dashed violet line), ZZ (large-dotted blue line), $h_d h_s$ (small-dotted red line) and $\chi_1 \chi_1$ (dot-dashed green line) vs. m_{h_p} . (d) Signal strengths of h_d in the ZZ channel (solid green line) and in the $\gamma\gamma$ channel (dashed red line) vs. m_{h_d} .

again, when one looks at the other BRs, shown in panel (e) against m_{h_s} . We see in the figure that $BR(h_p \rightarrow \chi_1 \chi_1)$ (solid cyan line) is always highly dominant. In fact for $\phi_\kappa = 0^\circ$ h_p almost always decays into a pair of χ_1 . With increasing ϕ_κ m_{h_s} starts falling and, consequently, $BR(h_p \rightarrow h_s h_s)$ (dashed violet line), starts rising. At the same time $BR(h_p \rightarrow W^+W^-)$ (large-dotted blue line) and $BR(h_p \rightarrow ZZ)$ (small-dotted orange line) also rise slowly, while $BR(h_p \rightarrow \chi_1 \chi_1)$ drops sharply, although it still remains the most dominant one for almost the entire allowed range of ϕ_κ . Only for $\phi_\kappa = 5^\circ$ the BR of hitherto the third dominant decay mode, $h_p \rightarrow W^+W^-$, rises slightly above the BRs of both $h_p \rightarrow \chi_1 \chi_1$ and $h_p \rightarrow h_s h_s$ and becomes the most dominant one, ~ 0.3 .

Finally, in panel (f) we show $R_{h_d}(\gamma\gamma)$ (solid red line) and $R_{h_d}(ZZ)$ (dashed green line) plotted against m_{h_d} for this case. We see that the mass of h_d falls quite sharply with increasing ϕ_κ , again in contrast with the earlier cases, which is one of the reasons for ϕ_κ being restricted to values of $\mathcal{O}(1)$, as noted earlier. Additionally, not only is $R_{h_d}(ZZ)$ considerably smaller than $R_{h_d}(\gamma\gamma)$ when CP is conserved, it also behaves quite differently with increasing ϕ_κ . $R_{h_d}(\gamma\gamma)$, already significantly above 1 in the CPC limit, slowly increases further with increasing ϕ_κ while $R_{h_d}(ZZ)$, also slightly above 1 initially, falls comparatively rapidly to become SM like at $\phi_\kappa = 5^\circ$. One may thus deduce in this case that non-zero values of ϕ_κ may already have been ruled out by the LHC Higgs boson data owing to its pushing $R_{h_d}(\gamma\gamma)$, which is already on the larger side in the CPC limit, upward. However, it should be noted that any further enhancement in the $\gamma\gamma$ rate is only slight with increasing ϕ_κ , so that it is still consistent with the ATLAS measurement, $\mu(\gamma\gamma) = 1.6 \pm 0.3$ [69]. On the other hand,

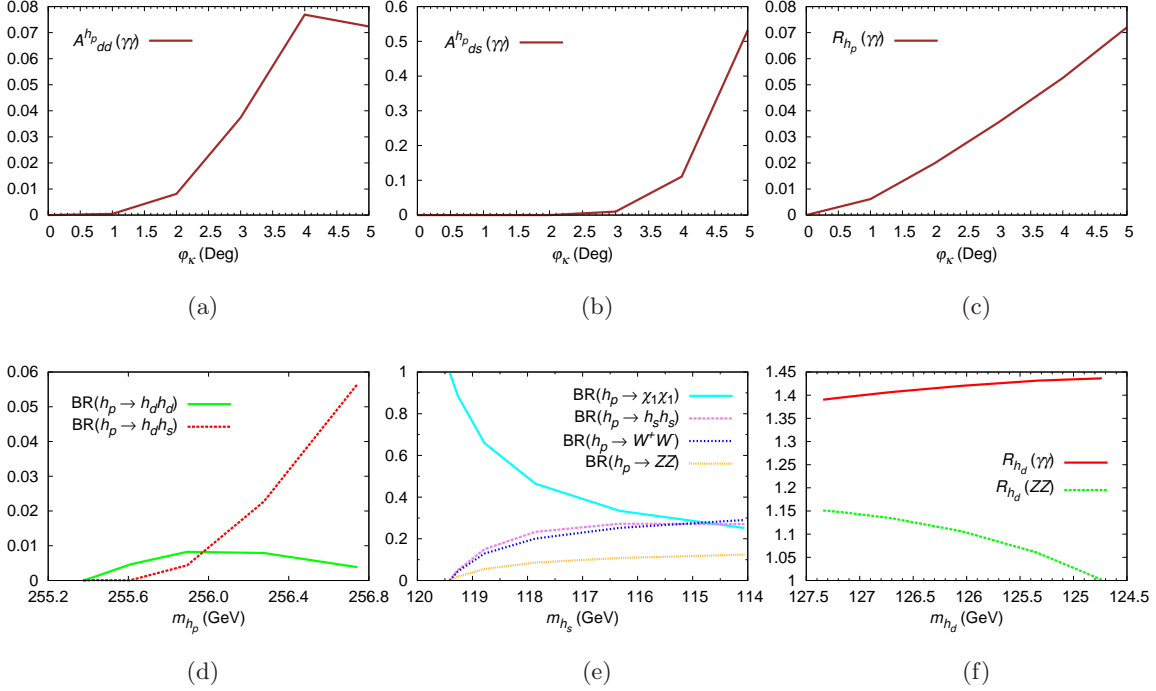


Figure 3: Case when $h_2 = h_d$ with large singlet-doublet mixing and $h_3 = h_p$. (a)–(c) Signal rates $A^{h_p}_{dd}(\gamma\gamma)$, $A^{h_p}_{ds}(\gamma\gamma)$ and $R_{h_p}(\gamma\gamma)$, respectively, as functions of ϕ_κ . (d) BRs of h_p into $h_d h_d$ (solid green line) and $h_d h_s$ (dashed red line) vs. m_{h_p} . (e) BRs of h_p into $\chi_1 \chi_1$ (solid cyan line), $h_s h_s$ (dashed violet line), $W^+ W^-$ (large-dotted blue line) and ZZ (small-dotted orange line) vs. m_{h_s} . (f) Signal strengths of h_d in the $\gamma\gamma$ channel (solid red line) and in the ZZ channel (dashed green line) vs. m_{h_d} .

non-zero values of ϕ_κ also yield $R_{h_d}(ZZ)$ closer to 1, and hence more SM-like, than in the CPC limit.

6 Summary and outlook

In this article we have presented the complete one-loop Higgs mass matrix of the complex NMSSM in the RG improved effective potential approach, along with the expressions for Higgs boson trilinear self-couplings. We have then highlighted a scenario, precluded in the MSSM, wherein the decay of a pseudoscalar-like Higgs boson into 125 GeV Higgs bosons is induced by non-zero values of the CPV phase ϕ_κ . We have noted that, when one of the scalar Higgs bosons is required to have SM-like signal rate, it is relatively easy for the mass of the singlet-pseudoscalar-like Higgs boson to be near ~ 250 GeV compared to the other heavy Higgs bosons of the model. The fact that the decay width of a heavy Higgs boson into two lighter ones is inversely proportional its mass renders such a ~ 250 GeV Higgs boson particularly interesting as well as relevant for the phenomenology of the SM-like Higgs boson in the model.

We have analysed three benchmark cases corresponding to different parameter configurations in the NMSSM which generate a ~ 125 GeV SM-like Higgs boson and a pseudoscalar near 250 GeV. In our analysis the impact of non-zero CPV phases in each of these cases is quantified in terms of an auxiliary signal rate $A^{h_p}(\gamma\gamma)$. This approximate quantity assumes that the ~ 250 GeV

pseudoscalar-like Higgs boson is produced in the gluon fusion mode at the LHC and decays into a (pair of) SM-like Higgs boson(s) which subsequently decays into photon pairs. By calculating this auxiliary rate in each case studied, we have deduced that such a ~ 250 GeV Higgs boson can generally contribute significantly to the production of SM-like Higgs bosons at the LHC for large CPV phases. In fact, in one of the cases discussed, the auxiliary signal rate for this Higgs boson can reach as high as about 50% of the signal strength in the $\gamma\gamma$ channel due to the production of the SM-like Higgs boson itself via gluon fusion.

Evidently, a calculation of the total cross section for our considered process is essential to draw concrete inferences about its observability or significance at the LHC. In this regard, a calculation of higher order corrections to the Higgs trilinear couplings in the complex NMSSM, following those derived in [73] for the real NMSSM, could prove crucial. Furthermore, a detailed study of the signal topologies in various channels due to the production of multiple Higgs bosons, in line with the ones studied recently in [72, 74, 75], is also in order. For this purpose, we eventually aim to embed the cNMSSM in a publicly available tool such as CalcHEP [76] to make possible the calculation of actual cross sections in this model. Our current analysis, nevertheless, serves as a clear and timely demonstration of the fact that CPV in the Higgs sector can be a very important probe of new physics at the LHC. Of particular relevance here is the observation that the ~ 250 GeV Higgs boson mostly has a very poor signal strength when decaying itself into a photon pair but a large BR into lighter Higgs bosons for non-zero CPV phases. Thus, the already observed SM-like Higgs boson could provide an important, and possibly only, handle on such a beyond the SM (and MSSM) scenario.

Acknowledgements

S. Munir is funded in part by the Welcome Programme of the Foundation for Polish Science.

A Sparticle mass matrices

- The chargino mass matrix, in the $(\tilde{W}^-, \tilde{H}^-)$ basis, using the convention $\tilde{H}_{L(R)}^- = \tilde{H}_{d(u)}^-$, can be written as

$$\mathcal{M}_C = \begin{pmatrix} M_2 & \sqrt{2}M_W \cos \beta \\ \sqrt{2}M_W \sin \beta & \frac{|\lambda|v_S}{\sqrt{2}} e^{i\phi'_\lambda} \end{pmatrix}, \quad (\text{A.1})$$

which is diagonalised by two different unitary matrices as $C_R \mathcal{M}_C C_L^\dagger = \text{diag}\{m_{\tilde{\chi}_1^\pm}, m_{\tilde{\chi}_2^\pm}\}$, where $m_{\tilde{\chi}_1^\pm} \leq m_{\tilde{\chi}_2^\pm}$.

- The neutralino mass matrix, in the $(\tilde{B}, \tilde{W}^0, \tilde{H}_d^0, \tilde{H}_u^0, \tilde{S})$ basis, can be written as

$$\mathcal{M}_N = \begin{pmatrix} M_1 & 0 & -m_Z \cos \beta s_W & m_Z \sin \beta s_W & 0 \\ & M_2 & m_Z \cos \beta c_W & -m_Z \sin \beta c_W & 0 \\ & & 0 & -\frac{|\lambda|v_S}{\sqrt{2}} e^{i\phi'_\lambda} & -\frac{|\lambda|v_S \beta}{\sqrt{2}} e^{i\phi'_\lambda} \\ & & & 0 & -\frac{|\lambda|v \cos \beta}{\sqrt{2}} e^{i\phi'_\lambda} \\ & & & & \sqrt{2}|\kappa|v_S e^{i\phi'_\kappa} \end{pmatrix}. \quad (\text{A.2})$$

It is diagonalised as $N^* \mathcal{M}_N N^\dagger = \text{diag} (m_{\tilde{\chi}_1^0}, m_{\tilde{\chi}_2^0}, m_{\tilde{\chi}_3^0}, m_{\tilde{\chi}_4^0}, m_{\tilde{\chi}_5^0})$, where N is a unitary matrix and $m_{\tilde{\chi}_1^0} \leq m_{\tilde{\chi}_2^0} \leq m_{\tilde{\chi}_3^0} \leq m_{\tilde{\chi}_4^0} \leq m_{\tilde{\chi}_5^0}$.

- For the stop, sbottom and stau matrices, in the $(\tilde{q}_L, \tilde{q}_R)$ basis, we have

$$\begin{aligned}\widetilde{\mathcal{M}}_t^2 &= \begin{pmatrix} M_{\tilde{Q}_3}^2 + m_t^2 + \cos 2\beta M_Z^2 (\frac{1}{2} - \frac{2}{3}s_W^2) & \frac{h_t^* v_u}{\sqrt{2}} (|A_t| e^{-i(\theta+\phi_{A_t})} - \frac{|\lambda| v_S}{\sqrt{2}} e^{i\phi'_\lambda} \cot \beta) \\ \frac{h_t v_u}{\sqrt{2}} (|A_t| e^{i(\theta+\phi_{A_t})} - \frac{|\lambda| v_S}{\sqrt{2}} e^{-i\phi'_\lambda} \cot \beta) & M_{\tilde{U}_3}^2 + m_t^2 + \cos 2\beta M_Z^2 Q_t s_W^2 \end{pmatrix}, \\ \widetilde{\mathcal{M}}_b^2 &= \begin{pmatrix} M_{\tilde{Q}_3}^2 + m_b^2 + \cos 2\beta M_Z^2 (-\frac{1}{2} + \frac{1}{3}s_W^2) & \frac{h_b^* v_d}{\sqrt{2}} (|A_b| e^{-i\phi_{A_b}} - \frac{|\lambda| v_S}{\sqrt{2}} e^{i\phi'_\lambda} \tan \beta) / \sqrt{2} \\ \frac{h_b v_d}{\sqrt{2}} (|A_b| e^{i\phi_{A_b}} - \frac{|\lambda| v_S}{\sqrt{2}} e^{-i\phi'_\lambda} \tan \beta) / \sqrt{2} & M_{\tilde{D}_3}^2 + m_b^2 + \cos 2\beta M_Z^2 Q_b s_W^2 \end{pmatrix}, \\ \widetilde{\mathcal{M}}_\tau^2 &= \begin{pmatrix} M_{\tilde{L}_3}^2 + m_\tau^2 + \cos 2\beta M_Z^2 (s_W^2 - 1/2) & \frac{h_\tau^* v_d}{\sqrt{2}} (|A_\tau| e^{-i\phi_{A_\tau}} - \frac{|\lambda| v_S}{\sqrt{2}} e^{i\phi'_\lambda} \tan \beta) / \sqrt{2} \\ \frac{h_\tau v_d}{\sqrt{2}} (|A_\tau| e^{i\phi_{A_\tau}} - \frac{|\lambda| v_S}{\sqrt{2}} e^{-i\phi'_\lambda} \tan \beta) / \sqrt{2} & M_{\tilde{E}_3}^2 + m_\tau^2 - \cos 2\beta M_Z^2 s_W^2 \end{pmatrix},\end{aligned}\tag{A.3}$$

where y_τ and m_τ are the mass and Yukawa coupling of the τ lepton, respectively, and $s_W = \sin \theta_W$. The mass eigenstates of top and bottom squarks and stau are obtained by diagonalising the above mass matrices as $U^{\tilde{f}\dagger} \widetilde{\mathcal{M}}_f^2 U^{\tilde{f}} = \text{diag}(m_{\tilde{f}_1}^2, m_{\tilde{f}_2}^2)$, such that $m_{\tilde{f}_1}^2 \leq m_{\tilde{f}_2}^2$, for $f = t, b$ and τ .

B Functions

- The functions used in the leading (s)quark corrections to the Higgs mass matrix are given as

$$\begin{aligned}L_{\tilde{t}} &= \ln \left(\frac{m_{\tilde{t}_2}^2}{m_{\tilde{t}_1}^2} \right), \quad L_{\tilde{b}} = \ln \left(\frac{m_{\tilde{b}_2}^2}{m_{\tilde{b}_1}^2} \right), \\ L_{\tilde{t}\tilde{t}} &= \ln \left(\frac{m_{\tilde{t}_1} m_{\tilde{t}_2}}{m_t^2} \right), \quad L_{\tilde{b}\tilde{b}} = \ln \left(\frac{m_{\tilde{b}_1} m_{\tilde{b}_2}}{m_b^2} \right), \\ f_t &= \frac{1}{m_{\tilde{t}_2}^2 - m_{\tilde{t}_1}^2} \left[m_{\tilde{t}_2}^2 \ln \left(\frac{m_{\tilde{t}_2}^2}{M_{\text{SUSY}}^2} \right) - m_{\tilde{t}_1}^2 \ln \left(\frac{m_{\tilde{t}_1}^2}{M_{\text{SUSY}}^2} \right) \right] - 1, \\ f_b &= \frac{1}{m_{\tilde{b}_2}^2 - m_{\tilde{b}_1}^2} \left[m_{\tilde{b}_2}^2 \ln \left(\frac{m_{\tilde{b}_2}^2}{M_{\text{SUSY}}^2} \right) - m_{\tilde{b}_1}^2 \ln \left(\frac{m_{\tilde{b}_1}^2}{M_{\text{SUSY}}^2} \right) \right] - 1, \\ g_t &= \left[\frac{m_{\tilde{t}_2}^2 + m_{\tilde{t}_1}^2}{m_{\tilde{t}_2}^2 - m_{\tilde{t}_1}^2} L_{\tilde{t}} - 2 \right], \quad g_b = \left[\frac{m_{\tilde{b}_2}^2 + m_{\tilde{b}_1}^2}{m_{\tilde{b}_2}^2 - m_{\tilde{b}_1}^2} L_{\tilde{b}} - 2 \right],\end{aligned}\tag{B.1}$$

where the mass eigenvalues $m_{\tilde{q}}$ have been given in Appendix A.

- Additional quantities used in the D -term contributions are given as

$$\begin{aligned}
g_u &= \frac{1}{4}g_2^2 - \frac{5}{12}g_1^2, \quad g_d = \frac{1}{4}g_2^2 - \frac{1}{12}g_1^2, \\
D_u &= \frac{1}{2}\left(M_{\tilde{Q}_3} - M_{\tilde{U}_3} + \frac{g_u}{2}(v_d^2 - v_u^2)\right), \\
D_d &= \frac{1}{2}\left(M_{\tilde{Q}_3} - M_{\tilde{D}_3} + \frac{g_d}{2}(v_u^2 - v_d^2)\right), \\
C_t &= \frac{3m_t^2}{32\pi^2} \left[\frac{4g_u D_u}{(m_{\tilde{t}_2}^2 - m_{\tilde{t}_1}^2)^2} g'_t - \frac{g_1^2 + g_2^2}{2(m_{\tilde{t}_2}^2 - m_{\tilde{t}_1}^2)} L_{\tilde{t}} \right], \\
C_b &= \frac{3m_b^2}{32\pi^2} \left[\frac{4g_d D_d}{(m_{\tilde{b}_2}^2 - m_{\tilde{b}_1}^2)^2} g'_b - \frac{g_1^2 + g_2^2}{2(m_{\tilde{b}_2}^2 - m_{\tilde{b}_1}^2)} L_{\tilde{b}} \right], \\
D_t &= -\frac{3m_t^2}{16\pi^2} \left[\frac{2g_u D_u}{(m_{\tilde{t}_2}^2 - m_{\tilde{t}_1}^2)} L_{\tilde{t}} + \frac{g_1^2 + g_2^2}{4} \ln \left(\frac{m_{\tilde{t}_1}^2 m_{\tilde{t}_2}^2}{M_{\text{SUSY}}^2} \right) \right], \\
D_b &= -\frac{3m_b^2}{16\pi^2} \left[\frac{2g_d D_d}{(m_{\tilde{b}_2}^2 - m_{\tilde{b}_1}^2)} L_{\tilde{b}} + \frac{g_1^2 + g_2^2}{4} \ln \left(\frac{m_{\tilde{b}_1}^2 m_{\tilde{b}_2}^2}{M_{\text{SUSY}}^2} \right) \right].
\end{aligned} \tag{B.2}$$

- The chargino/neutralino corrections use the following potentially large logarithms:

$$\begin{aligned}
L_\mu &= \ln \left(\frac{|\mu|^2}{M_{\text{SUSY}}^2} \right), \quad L_\nu = \ln \left(\frac{4|\nu|^2}{M_{\text{SUSY}}^2} \right), \\
L_{M_{2\mu}} &= \ln \left(\frac{\max(M_{1,2}^2, |\mu|^2)}{M_{\text{SUSY}}^2} \right), \quad L_{\mu\nu} = \ln \left(\frac{\max(4|\nu|^2, |\mu|^2)}{M_{\text{SUSY}}^2} \right),
\end{aligned} \tag{B.3}$$

where for simplification we assume $M_1 \sim M_2 \equiv M_{1,2}$ for the gaugino masses.

- The Higgs wave function renormalisation constants for the three weak eigenstates H_u , H_d and S are given, in the Landau gauge, as

$$\begin{aligned}
Z_{H_u} &= 1 + \frac{1}{16\pi^2} \left[3h_t^2 \ln \left(\frac{M_{\text{SUSY}}^2}{m_t^2} \right) - \frac{3}{4}(g_1^2 + 3g_2^2) \ln \left(\frac{M_{\text{SUSY}}^2}{m_Z^2} \right) \right. \\
&\quad + \cos^2 \left[3h_b^2 + h_\tau^2 - 3h_t^2 \right] \ln \left(\frac{M_A^2}{m_t^2} \right) + \frac{g_1^2}{2} \ln \left(\frac{M_{\text{SUSY}}^2}{\max(|\mu|^2, M_1^2)} \right) \\
&\quad \left. + \frac{3g_2^2}{2} \ln \left(\frac{M_{\text{SUSY}}^2}{\max(|\mu|^2, M_2^2)} \right) + \lambda^2 \ln \left(\frac{M_{\text{SUSY}}^2}{\max(|\mu|^2, 4|\nu|^2)} \right) \right], \\
Z_{H_d} &= 1 + \frac{1}{16\pi^2} \left[(3h_b^2 + h_\tau^2) \ln \left(\frac{M_{\text{SUSY}}^2}{m_t^2} \right) - \frac{3}{4}(g_1^2 + 3g_2^2) \ln \left(\frac{M_{\text{SUSY}}^2}{m_Z^2} \right) \right. \\
&\quad + \sin^2 \left[3h_t^2 - h_\tau^2 - 3h_b^2 \right] \ln \left(\frac{M_A^2}{m_t^2} \right) + \frac{g_1^2}{2} \ln \left(\frac{M_{\text{SUSY}}^2}{\max(|\mu|^2, M_1^2)} \right) \\
&\quad \left. + \frac{3g_2^2}{2} \ln \left(\frac{M_{\text{SUSY}}^2}{\max(|\mu|^2, M_2^2)} \right) + l^2 \ln \left(\frac{M_{\text{SUSY}}^2}{\max(|\mu|^2, 4|\nu|^2)} \right) \right], \\
Z_S &= 1 + \frac{1}{8\pi^2} \left[\lambda^2 \ln \left(\frac{M_{\text{SUSY}}^2}{|\mu|^2} \right) + \kappa^2 \ln \left(\frac{M_{\text{SUSY}}^2}{4|\nu|^2} \right) \right].
\end{aligned} \tag{B.4}$$

References

- [1] **ATLAS Collaboration** Collaboration, G. Aad *et al.*, “Observation of a new particle in the search for the Standard Model Higgs boson with the ATLAS detector at the LHC,” [arXiv:1207.7214 \[hep-ex\]](#).
- [2] **CMS Collaboration** Collaboration, S. Chatrchyan *et al.*, “Observation of a new boson at a mass of 125 GeV with the CMS experiment at the LHC,” [arXiv:1207.7235 \[hep-ex\]](#).
- [3] S. Meola, “Measurements of properties of the Higgs-like Particle at 125 GeV by the CMS collaboration,” [arXiv:1310.4146 \[hep-ex\]](#).
- [4] <https://twiki.cern.ch/twiki/bin/view/CMSPublic/PhysicsResultsHIG>
- [5] <https://twiki.cern.ch/twiki/bin/view/AtlasPublic/HiggsPublicResults>
- [6] J. Christenson, J. Cronin, V. Fitch, and R. Turlay, “Evidence for the 2 pi Decay of the $k(2)0$ Meson,” *Phys.Rev.Lett.* **13** (1964) 138–140.
- [7] M. Kobayashi and T. Maskawa, “CP Violation in the Renormalizable Theory of Weak Interaction,” *Prog.Theor.Phys.* **49** (1973) 652–657.
- [8] T. Ibrahim and P. Nath, “CP Violation From Standard Model to Strings,” *Rev.Mod.Phys.* **80** (2008) 577–631, [arXiv:0705.2008 \[hep-ph\]](#).
- [9] A. Pilaftsis, “CP odd tadpole renormalization of Higgs scalar - pseudoscalar mixing,” *Phys.Rev.* **D58** (1998) 096010, [arXiv:hep-ph/9803297 \[hep-ph\]](#).
- [10] A. Pilaftsis, “Higgs scalar - pseudoscalar mixing in the minimal supersymmetric standard model,” *Phys.Lett.* **B435** (1998) 88–100, [arXiv:hep-ph/9805373 \[hep-ph\]](#).
- [11] A. Pilaftsis and C. E. Wagner, “Higgs bosons in the minimal supersymmetric standard model with explicit CP violation,” *Nucl.Phys.* **B553** (1999) 3–42, [arXiv:hep-ph/9902371 \[hep-ph\]](#).
- [12] S. Choi, M. Drees, and J. S. Lee, “Loop corrections to the neutral Higgs boson sector of the MSSM with explicit CP violation,” *Phys.Lett.* **B481** (2000) 57–66, [arXiv:hep-ph/0002287 \[hep-ph\]](#).
- [13] M. S. Carena, J. R. Ellis, A. Pilaftsis, and C. Wagner, “Renormalization group improved effective potential for the MSSM Higgs sector with explicit CP violation,” *Nucl.Phys.* **B586** (2000) 92–140, [arXiv:hep-ph/0003180 \[hep-ph\]](#).
- [14] M. S. Carena, J. R. Ellis, A. Pilaftsis, and C. Wagner, “Higgs boson pole masses in the MSSM with explicit CP violation,” *Nucl.Phys.* **B625** (2002) 345–371, [arXiv:hep-ph/0111245 \[hep-ph\]](#).
- [15] M. S. Carena, J. R. Ellis, S. Mrenna, A. Pilaftsis, and C. Wagner, “Collider probes of the MSSM Higgs sector with explicit CP violation,” *Nucl.Phys.* **B659** (2003) 145–178, [arXiv:hep-ph/0211467 \[hep-ph\]](#).
- [16] S. Choi, J. Kalinowski, Y. Liao, and P. Zerwas, “H/A Higgs mixing in CP-noninvariant supersymmetric theories,” *Eur.Phys.J.* **C40** (2005) 555–564, [arXiv:hep-ph/0407347 \[hep-ph\]](#).

- [17] D. A. Demir, “Effects of the supersymmetric phases on the neutral Higgs sector,” *Phys.Rev.* **D60** (1999) 055006, [arXiv:hep-ph/9901389](#) [hep-ph].
- [18] G. L. Kane and L.-T. Wang, “Implications of supersymmetry phases for Higgs boson signals and limits,” *Phys.Lett.* **B488** (2000) 383–389, [arXiv:hep-ph/0003198](#) [hep-ph].
- [19] M. S. Carena, J. R. Ellis, A. Pilaftsis, and C. Wagner, “CP violating MSSM Higgs bosons in the light of LEP-2,” *Phys.Lett.* **B495** (2000) 155–163, [arXiv:hep-ph/0009212](#) [hep-ph].
- [20] A. Arhrib, D. K. Ghosh, and O. C. Kong, “Observing CP violating MSSM Higgs bosons at hadron colliders?,” *Phys.Lett.* **B537** (2002) 217–226, [arXiv:hep-ph/0112039](#) [hep-ph].
- [21] S. Choi, K. Hagiwara, and J. S. Lee, “Higgs boson decays in the minimal supersymmetric standard model with radiative Higgs sector CP violation,” *Phys.Rev.* **D64** (2001) 032004, [arXiv:hep-ph/0103294](#) [hep-ph].
- [22] S. Choi, M. Drees, J. S. Lee, and J. Song, “Supersymmetric Higgs boson decays in the MSSM with explicit CP violation,” *Eur.Phys.J.* **C25** (2002) 307–313, [arXiv:hep-ph/0204200](#) [hep-ph].
- [23] J. R. Ellis, J. S. Lee, and A. Pilaftsis, “Resonant CP violation in Higgs radiation at e+ e- linear collider,” *Phys.Rev.* **D72** (2005) 095006, [arXiv:hep-ph/0507046](#) [hep-ph].
- [24] V. Cirigliano, Y. Li, S. Profumo, and M. J. Ramsey-Musolf, “MSSM Baryogenesis and Electric Dipole Moments: An Update on the Phenomenology,” *JHEP* **1001** (2010) 002, [arXiv:0910.4589](#) [hep-ph].
- [25] C. Baker, D. Doyle, P. Geltenbort, K. Green, M. van der Grinten, *et al.*, “An Improved experimental limit on the electric dipole moment of the neutron,” *Phys.Rev.Lett.* **97** (2006) 131801, [arXiv:hep-ex/0602020](#) [hep-ex].
- [26] E. D. Commins, “Electric dipole moments of elementary particles, nuclei, atoms, and molecules,” *J.Phys.Soc.Jap.* **76** (2007) 111010.
- [27] W. Griffith, M. Swallows, T. Loftus, M. Romalis, B. Heckel, *et al.*, “Improved Limit on the Permanent Electric Dipole Moment of Hg-199,” *Phys.Rev.Lett.* **102** (2009) 101601.
- [28] A. Dedes and S. Moretti, “Effect of large supersymmetric phases on Higgs production,” *Phys.Rev.Lett.* **84** (2000) 22–25, [arXiv:hep-ph/9908516](#) [hep-ph].
- [29] A. Dedes and S. Moretti, “Effects of CP violating phases on Higgs boson production at hadron colliders in the minimal supersymmetric standard model,” *Nucl.Phys.* **B576** (2000) 29–55, [arXiv:hep-ph/9909418](#) [hep-ph].
- [30] S. Choi, K. Hagiwara, and J. S. Lee, “Observability of the lightest MSSM Higgs boson with explicit CP violation via gluon fusion at the LHC,” *Phys.Lett.* **B529** (2002) 212–221, [arXiv:hep-ph/0110138](#) [hep-ph].
- [31] J. R. Ellis, J. S. Lee, and A. Pilaftsis, “CERN LHC signatures of resonant CP violation in a minimal supersymmetric Higgs sector,” *Phys.Rev.* **D70** (2004) 075010, [arXiv:hep-ph/0404167](#) [hep-ph].
- [32] S. Moretti, S. Munir, and P. Poulose, “Explicit CP Violation in the MSSM Through Higgs $\rightarrow \gamma\gamma$,” *Phys.Lett.* **B649** (2007) 206–211, [arXiv:hep-ph/0702242](#) [HEP-PH].

- [33] S. Hesselbach, S. Moretti, S. Munir, and P. Poulose, “Exploring the Di-Photon Decay of a Light Higgs Boson in the MSSM With Explicit CP Violation,” *Eur.Phys.J.* **C54** (2008) 129–147, [arXiv:0706.4269 \[hep-ph\]](#).
- [34] S. Hesselbach, S. Moretti, S. Munir, and P. Poulose, “Explicit CP violation in the MSSM through $gg \rightarrow H \rightarrow \gamma\gamma$,” *Phys.Rev.* **D82** (2010) 074004, [arXiv:0903.0747 \[hep-ph\]](#).
- [35] A. Chakraborty, B. Das, J. L. Diaz-Cruz, D. K. Ghosh, S. Moretti, *et al.*, “The 125 GeV Higgs signal at the LHC in the CP Violating MSSM,” [arXiv:1301.2745 \[hep-ph\]](#).
- [36] M. Drees, “Supersymmetric Models with Extended Higgs Sector,” *Int.J.Mod.Phys.* **A4** (1989) 3635.
- [37] J. R. Ellis, J. Gunion, H. E. Haber, L. Roszkowski, and F. Zwirner, “Higgs Bosons in a Nonminimal Supersymmetric Model,” *Phys.Rev.* **D39** (1989) 844.
- [38] U. Ellwanger, C. Hugonie, and A. M. Teixeira, “The Next-to-Minimal Supersymmetric Standard Model,” *Phys.Rept.* **496** (2010) 1–77, [arXiv:0910.1785 \[hep-ph\]](#).
- [39] M. Maniatis, “The Next-to-Minimal Supersymmetric extension of the Standard Model reviewed,” *Int.J.Mod.Phys.* **A25** (2010) 3505–3602, [arXiv:0906.0777 \[hep-ph\]](#).
- [40] U. Ellwanger, “A Higgs boson near 125 GeV with enhanced di-photon signal in the NMSSM,” *JHEP* **1203** (2012) 044, [arXiv:1112.3548 \[hep-ph\]](#).
- [41] J. F. Gunion, Y. Jiang, and S. Kraml, “Could two NMSSM Higgs bosons be present near 125 GeV?,” *Phys.Rev.* **D86** (2012) 071702, [arXiv:1207.1545 \[hep-ph\]](#).
- [42] S. Munir, L. Roszkowski, and S. Trojanowski, “Simultaneous enhancement in $\gamma\gamma$, $b\bar{b}$ and $\tau^+\tau^-$ rates in the NMSSM with nearly degenerate scalar and pseudoscalar Higgs bosons,” *Phys. Rev.* **D88** (2013) 055017, [arXiv:1305.0591 \[hep-ph\]](#).
- [43] S. Moretti, S. Munir, and P. Poulose, “The 125 GeV Higgs Boson signal within the Complex NMSSM,” [arXiv:1305.0166 \[hep-ph\]](#).
- [44] S. Abel, S. Khalil, and O. Lebedev, “EDM constraints in supersymmetric theories,” *Nucl.Phys.* **B606** (2001) 151–182, [arXiv:hep-ph/0103320 \[hep-ph\]](#).
- [45] N. Haba, “Explicit CP violation in the Higgs sector of the next-to-minimal supersymmetric standard model,” *Prog.Theor.Phys.* **97** (1997) 301–310, [arXiv:hep-ph/9608357 \[hep-ph\]](#).
- [46] T. Ibrahim and P. Nath, “The Neutron and the lepton EDMs in MSSM, large CP violating phases, and the cancellation mechanism,” *Phys.Rev.* **D58** (1998) 111301, [arXiv:hep-ph/9807501 \[hep-ph\]](#).
- [47] M. Boz, “The Higgs sector and electron electric dipole moment in next-to-minimal supersymmetry with explicit CP violation,” *Mod.Phys.Lett.* **A21** (2006) 243–264, [arXiv:hep-ph/0511072 \[hep-ph\]](#).
- [48] J. R. Ellis, J. S. Lee, and A. Pilaftsis, “Electric Dipole Moments in the MSSM Reloaded,” *JHEP* **0810** (2008) 049, [arXiv:0808.1819 \[hep-ph\]](#).

- [49] Y. Li, S. Profumo, and M. Ramsey-Musolf, “A Comprehensive Analysis of Electric Dipole Moment Constraints on CP-violating Phases in the MSSM,” *JHEP* **1008** (2010) 062, [arXiv:1006.1440 \[hep-ph\]](#).
- [50] S. Ham, S. Oh, and D. Son, “Neutral Higgs sector of the next-to-minimal supersymmetric standard model with explicit CP violation,” *Phys.Rev.* **D65** (2002) 075004, [arXiv:hep-ph/0110052 \[hep-ph\]](#).
- [51] K. Funakubo and S. Tao, “The Higgs sector in the next-to-MSSM,” *Prog.Theor.Phys.* **113** (2005) 821–842, [arXiv:hep-ph/0409294 \[hep-ph\]](#).
- [52] K. Cheung, T.-J. Hou, J. S. Lee, and E. Senaha, “The Higgs Boson Sector of the Next-to-MSSM with CP Violation,” *Phys.Rev.* **D82** (2010) 075007, [arXiv:1006.1458 \[hep-ph\]](#).
- [53] T. Graf, R. Grober, M. Muhlleitner, H. Rzehak, and K. Walz, “Higgs Boson Masses in the Complex NMSSM at One-Loop Level,” *JHEP* **1210** (2012) 122, [arXiv:1206.6806 \[hep-ph\]](#).
- [54] <http://www.th.u-psud.fr/NMHDECAY/nmssmtools.html>
- [55] K. Cheung, T.-J. Hou, J. S. Lee, and E. Senaha, “Higgs Mediated EDMs in the Next-to-MSSM: An Application to Electroweak Baryogenesis,” *Phys.Rev.* **D84** (2011) 015002, [arXiv:1102.5679 \[hep-ph\]](#).
- [56] J. Lee, A. Pilaftsis, M. S. Carena, S. Choi, M. Drees, *et al.*, “CPsuperH: A Computational tool for Higgs phenomenology in the minimal supersymmetric standard model with explicit CP violation,” *Comput.Phys.Commun.* **156** (2004) 283–317, [arXiv:hep-ph/0307377 \[hep-ph\]](#).
- [57] M. Spira, “QCD effects in Higgs physics,” *Fortsch.Phys.* **46** (1998) 203–284, [arXiv:hep-ph/9705337 \[hep-ph\]](#).
- [58] M. Spira, A. Djouadi, D. Graudenz, and P. Zerwas, “Higgs boson production at the LHC,” *Nucl.Phys.* **B453** (1995) 17–82, [arXiv:hep-ph/9504378 \[hep-ph\]](#).
- [59] S. King, M. Muhlleitner, and R. Nevzorov, “NMSSM Higgs Benchmarks Near 125 GeV,” *Nucl.Phys.* **B860** (2012) 207–244, [arXiv:1201.2671 \[hep-ph\]](#).
- [60] J. F. Gunion, Y. Jiang, and S. Kraml, “The Constrained NMSSM and Higgs near 125 GeV,” *Phys.Lett.* **B710** (2012) 454–459, [arXiv:1201.0982 \[hep-ph\]](#).
- [61] U. Ellwanger and C. Hugonie, “Higgs bosons near 125 GeV in the NMSSM with constraints at the GUT scale,” *Adv.High Energy Phys.* **2012** (2012) 625389, [arXiv:1203.5048 \[hep-ph\]](#).
- [62] R. Benbrik, M. Gomez Bock, S. Heinemeyer, O. Stal, G. Weiglein, *et al.*, “Confronting the MSSM and the NMSSM with the Discovery of a Signal in the two Photon Channel at the LHC,” *Eur.Phys.J.* **C72** (2012) 2171, [arXiv:1207.1096 \[hep-ph\]](#).
- [63] S. King, M. Muhlleitner, R. Nevzorov, and K. Walz, “Natural NMSSM Higgs Bosons,” *Nucl.Phys.* **B870** (2013) 323–352, [arXiv:1211.5074 \[hep-ph\]](#).
- [64] K. Kowalska, S. Munir, L. Roszkowski, E. M. Sessolo, S. Trojanowski, *et al.*, “The Constrained NMSSM with a 125 GeV Higgs boson – A global analysis,” *Phys. Rev.* **D87** (2013) 115010, [arXiv:1211.1693 \[hep-ph\]](#).

- [65] T. Gherghetta, B. von Harling, A. D. Medina, and M. A. Schmidt, “The Scale-Invariant NMSSM and the 126 GeV Higgs Boson,” *JHEP* **1302** (2013) 032, [arXiv:1212.5243 \[hep-ph\]](#).
- [66] R. Barbieri, D. Buttazzo, K. Kannike, F. Sala, and A. Tesi, “Exploring the Higgs sector of a most natural NMSSM,” *Phys. Rev. D* **87**, **115018** (2013) , [arXiv:1304.3670 \[hep-ph\]](#).
- [67] M. Badziak, M. Olechowski, and S. Pokorski, “New Regions in the NMSSM with a 125 GeV Higgs,” *JHEP* **1306** (2013) 043, [arXiv:1304.5437 \[hep-ph\]](#).
- [68] “Combination of standard model higgs boson searches and measurements of the properties of the new boson with a mass near 125 gev,” Tech. Rep. CMS-PAS-HIG-13-005, CERN, Geneva, 2013
- [69] “Combined measurements of the mass and signal strength of the higgs-like boson with the atlas detector using up to 25/fb of proton-proton collision data,” Tech. Rep. ATLAS-CONF-2013-014, CERN, Geneva, Mar, 2013
- [70] **LEP Working Group for Higgs boson searches, ALEPH Collaboration, DELPHI Collaboration, L3 Collaboration, OPAL Collaboration** Collaboration, R. Barate *et al.*, “Search for the standard model Higgs boson at LEP,” *Phys.Lett.* **B565** (2003) 61–75, [arXiv:hep-ex/0306033 \[hep-ex\]](#).
- [71] **XENON100 Collaboration** Collaboration, E. Aprile *et al.*, “Dark Matter Results from 225 Live Days of XENON100 Data,” *Phys.Rev.Lett.* **109** (2012) 181301, [arXiv:1207.5988 \[astro-ph.CO\]](#).
- [72] Z. Kang, J. Li, T. Li, D. Liu, and J. Shu, “Probing the CP-even Higgs Sector via $H_3 \rightarrow H_2 H_1$ in the Natural NMSSM,” *Phys.Rev.* **D88** (2013) 015006, [arXiv:1301.0453 \[hep-ph\]](#).
- [73] D. T. Nhung, M. Muhlleitner, J. Streicher, and K. Walz, “Higher Order Corrections to the Trilinear Higgs Self-Couplings in the Real NMSSM,” [arXiv:1306.3926 \[hep-ph\]](#).
- [74] U. Ellwanger, “Higgs pair production in the NMSSM at the LHC,” *JHEP* **1308** (2013) 077, [arXiv:1306.5541 \[hep-ph\]](#).
- [75] J. M. No and M. Ramsey-Musolf, “Probing the Higgs Portal at the LHC Through Resonant di-Higgs Production,” [arXiv:1310.6035 \[hep-ph\]](#).
- [76] A. Belyaev, N. D. Christensen, and A. Pukhov, “CalcHEP 3.4 for collider physics within and beyond the Standard Model,” *Comput.Phys.Commun.* **184** (2013) 1729–1769, [arXiv:1207.6082 \[hep-ph\]](#).